

AD-A080 650

NAVAL OCEAN SYSTEMS CENTER SAN DIEGO CA

F/6 18/6

EMP HARDENING OF AIRBORNE SYSTEMS THROUGH ELECTRO-OPTICAL TECHN--ETC(U)

DEC 79 R A GREENWELL

UNCLASSIFIED

NOSC/TR-469

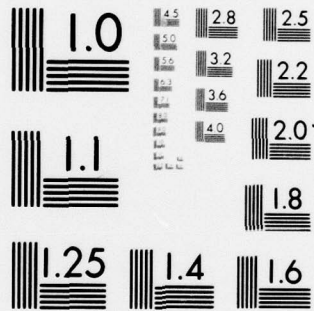
NL

OF
AD
A080650

NOSC



END
DATE
FILMED
3 - 80
DDC



MICROCOPY RESOLUTION TEST CHART
NATIONAL BUREAU OF STANDARDS-1963-A

LEVEL II

12 BS

NOSC

ADA 080650

NOSC TR 469

NOSC TR 469

Technical Report 469

EMP HARDENING OF AIRBORNE SYSTEMS THROUGH ELECTRO-OPTICAL TECHNIQUES: DESIGN GUIDELINES

RA Greenwell

15 December 1979

Research & Development: Apr — Aug 1979

Prepared for
Defense Nuclear Agency
RAEV
Alexandria, VA 20305

Approved for public release; distribution unlimited

NAVAL OCEAN SYSTEMS CENTER
SAN DIEGO, CALIFORNIA 92152

DDC
RECEIVED
FEB 14 1980
D

80 2 14 015

DDC FILE COPY



NAVAL OCEAN SYSTEMS CENTER, SAN DIEGO, CA 92152

AN ACTIVITY OF THE NAVAL MATERIAL COMMAND

SL GUILLE, CAPT, USN

Commander

HL BLOOD

Technical Director

ADMINISTRATIVE INFORMATION

Work was conducted under NOSC direction through contract N66001-79-C-0191 to Jaycor, Del Mar, CA, as part of the Guidelines for EMP Hardening Using Electro-Optic Techniques Program of the Defense Nuclear Agency (RAEV) under Program Element RDDA, work unit CG53. This report covers work from April to August 1979, and was approved for publication 15 December 1979.

Released by
LT RA Kraft
Air Surveillance Systems
Project Office

Under Authority of
RE Shuttles, Head
Surface/Aerospace
Surveillance Department

ACKNOWLEDGMENTS

The following were the major contributors at Jaycor to this effort:

WH Hardwick

DF Higgins

JF Leavy

This report is taken from contributions of these personnel.

UNCLASSIFIED

14 NOSC/TR-469

SECURITY CLASSIFICATION OF THIS PAGE (When Data Entered)

REPORT DOCUMENTATION PAGE		READ INSTRUCTIONS BEFORE COMPLETING FORM
1. REPORT NUMBER NOSC Technical Report 469 (TR 469) ✓	2. GOVT ACCESSION NO.	3. RECIPIENT'S CATALOG NUMBER
4. TITLE (and Subtitle) 6 EMP HARDENING OF AIRBORNE SYSTEMS THROUGH ELECTRO-OPTICAL TECHNIQUES: DESIGN GUIDELINES	5. TYPE OF REPORT & PERIOD COVERED R&D Apr to Aug 1979	
	6. PERFORMING ORG. REPORT NUMBER	
7. AUTHOR(s) RA Greenwell 10 R. A. / Greenwell	8. CONTRACT OR GRANT NUMBER(s) 12 55	
9. PERFORMING ORGANIZATION NAME AND ADDRESS Naval Ocean Systems Center ✓ San Diego, California 92152	10. PROGRAM ELEMENT, PROJECT, TASK AREA & WORK UNIT NUMBERS RDDA, CG53	
11. CONTROLLING OFFICE NAME AND ADDRESS Defense Nuclear Agency RAEV, Alexandria, VA 20305	12. REPORT DATE 11 15 December 1979	
	13. NUMBER OF PAGES 53	
14. MONITORING AGENCY NAME & ADDRESS (if different from Controlling Office) 9 Technical rept. Apr - Aug 79	15. SECURITY CLASS. (of this report) Unclassified	
	15a. DECLASSIFICATION/DOWNGRADING SCHEDULE	
16. DISTRIBUTION STATEMENT (of this Report) Approved for public release; distribution unlimited		
17. DISTRIBUTION STATEMENT (of the abstract entered in Block 20, if different from Report)		
18. SUPPLEMENTARY NOTES		
19. KEY WORDS (Continue on reverse side if necessary and identify by block number) Communication equipment - Hardening Fiber optics Control systems - Hardening Hardening Electromagnetic pulse (EMP) Optical materials Electromagnetic shielding Radiation hardening		
20. ABSTRACT (Continue on reverse side if necessary and identify by block number) Examines the utilization of fiber optics technology as an alternative to system EMP hardening and provides design guidelines for airborne system applications. Examines potential EMP vulnerabilities of the overall fiber optic data subsystems, defines and quantifies methods of protection against the EMP threat, and compares vulnerabilities with those of hard-wired data systems.		

DD FORM 1 JAN 73 1473

EDITION OF 1 NOV 65 IS OBSOLETE
S/N 0102 LF 014 6601

UNCLASSIFIED

SECURITY CLASSIFICATION OF THIS PAGE (When Data Entered)

393 159

JCB

OBJECTIVE

Provide design guidelines for EMP hardening of airborne transmission lines by use of optical fiber techniques.

RESULTS

1. Adequate protection can be provided to reduce the coupled signals below the burnout and upset threshold levels for the typical integrated circuit families that are used in the implementation of EO data systems.
2. In the case of data systems with long transmission path lengths (greater than 20 m), it will be easier to provide the required EMP protection for EO systems than for hard-wire systems.
3. A single-fiber connector will provide more attenuation than a bundle connector.

RECOMMENDATIONS

1. For systems in which significant EMP fields are present at electronics box interfaces and which cannot tolerate upsets in the receiver electronics, use the single-fiber approach in the system design.
2. If the system design is committed to fiber optic bundle technology, pigtail the photodetector and locate it physically away from the end of the panel mount connector to decrease receiver upset vulnerability to EMP.
3. If power must be distributed to the chassis containing EO transmitters and receivers through relatively long conductors, provide extra filtering on the power supply to keep the EMP-induced transients on the power supply and ground conductors from causing upsets.

Accession For	
NTIS GRI&I	<input checked="" type="checkbox"/>
DDC TAB	<input type="checkbox"/>
Unannounced	<input type="checkbox"/>
Justification	
By _____	
Distribution/	
Availability Codes	
Dist.	Avail and/or special
A	

CONTENTS

INTRODUCTION . . .	page 3
ELECTROMAGNETIC COUPLING IN AIRBORNE SYSTEMS . . .	7
FIBER OPTIC SUSCEPTIBILITIES TO EMP . . .	18
Burnout susceptibilities . . .	18
Upsets . . .	21
Fiber optic transmitter susceptibilities to EMP . . .	24
Fiber optic receiver susceptibilities to EMP . . .	25
EMP considerations related to the power supply distribution system for fiber optic systems . . .	28
EMP HARDENING TECHNIQUES . . .	29
Electromagnetic shielding . . .	29
Upset protection . . .	33
Shielding requirement estimates . . .	33
ELECTRO-OPTIC SYSTEM SUSCEPTIBILITY ANALYSIS . . .	35
CONCLUSIONS AND RECOMMENDATIONS . . .	38
REFERENCES . . .	39
APPENDIX A. ESTIMATES OF CABLE COUPLING . . .	41
APPENDIX B. ELECTROMAGNETIC SHIELDING . . .	43
APPENDIX C. EM COUPLING THROUGH FIBER OPTIC CONNECTORS . . .	51

INTRODUCTION

Electronics has become increasingly more sophisticated, and because integrated circuits and new electronic devices operate at even lower power levels, electronic systems have also become more susceptible to damage or upset from transients such as electromagnetic pulse (EMP).

The Defense Department is interested in optical fiber data interfaces for airborne system applications because of the inherent advantages of a dielectric waveguide in an electromagnetic environment. This report examines the utilization of fiber optics (FO) technology as an alternative to system EMP hardening and provides design guidelines for airborne system applications. Potential EMP vulnerabilities of the overall FO data subsystems are examined for airborne systems. Where susceptibilities are identified, methods of protection against the EMP threat are defined and quantified. Vulnerabilities are compared to those of hard-wired data systems.

Currently available information was used in identifying and analyzing these vulnerabilities. As fiber optic technology matures and experience is gained in the design and operation of these systems, it is certain that other susceptibilities will be identified and different methods of analyzing them developed.

Potential applications for electro-optical (EO) techniques in the transmitting of data in military aircraft are numerous and varied. At the present state of development of the technology, it is feasible to replace most hard-wired data transmission systems with EO systems. Typical interface characteristics are shown in figure 1. However, electro-optical systems are limited to those applications in which signal processing and/or transmission are the primary objectives. Electro-optical techniques are well suited to performing functions in analog as well as digital signal processing.

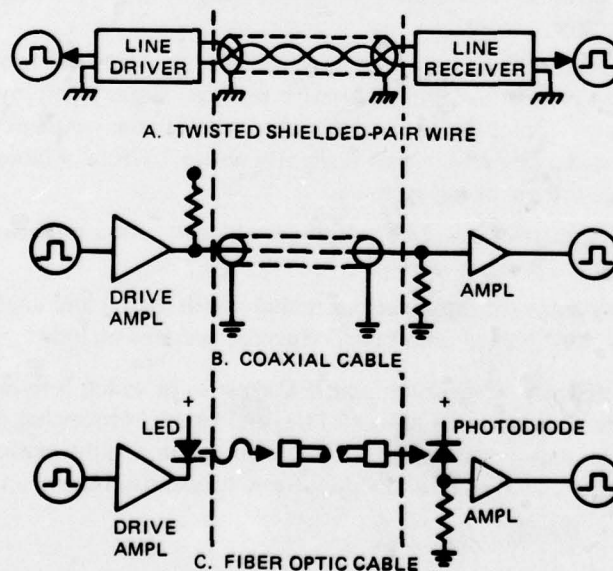


Figure 1. Typical interface systems.

The possible threat to aircraft posed by EMP is a problem that has been increasingly recognized over the past few years. As a result, numerous analysis tools and hardening techniques have been developed and investigated. Similarly, EMP simulators have been built and several actual aircraft have been tested and their EMP vulnerabilities evaluated. Furthermore, this effort to obtain EMP-hardened aircraft is likely to continue, since more sophisticated and sensitive electronics are always being added to newer aeronautical systems.

In recent years there have also been numerous advances in the capabilities of fiber optic data systems. Some such systems are now becoming competitive with hard-wired data systems in terms of reliability and cost. As a result, such EO techniques have been tested on aircraft systems and may soon be used on operational aircraft.

Another major reason for considering fiber optic data systems for military applications is a potential reduction in EMP susceptibility. However, without careful consideration, the replacement of hard-wired data paths with fiber optic systems may not result in EMP susceptibility improvement. This document discusses the susceptibility of fiber optics data systems relative to hard-wired systems, and presents some design approaches and guidelines for EMP hardening of systems.

Potential EMP vulnerabilities of the overall fiber optic system will be examined, and where susceptibilities are identified, methods of protection against the EMP threat will be defined and quantified where possible. Vulnerabilities will be compared to those of hard-wired data systems if possible.

Currently available information was used in identifying and analyzing these vulnerabilities. As the fiber optic technology grows and matures and more experience is gained in the design and operation of these systems, it is certain that other susceptibilities will be identified and different methods of analyzing them developed.

Potential applications of EO techniques to the transmitting of data in military aircraft systems are numerous and varied. At the present state of development of the technology, it is feasible to replace most hard-wired data transmission systems with EO systems. However, EO systems are limited to those applications in which signal processing and/or transmission are the primary objectives.

If it is required that relatively high power levels (>10 mW) be transmitted as well, EO systems are not at present a viable alternative to those already employed, such as coaxial and microwave systems. Practical upper limits also exist for the frequency at which the light may be modulated. At present, this is slightly above 1 GHz for laboratory devices and in the 500-MHz range for operating systems.

With these few restrictions, EO techniques are well suited to performing functions in analog as well as digital signal processing.

In airborne systems, the applications include both digital and analog point-to-point data links, as well as multiplexed data buses. Specific systems include:

- Weapons delivery, navigation, and IFF systems in which interconnections are made between remote terminal units (RTUs) and central processing units (CPUs). These systems can require both digital data, such as command, control, and timing, and analog signals, such as IF and video, to be transmitted between RTUs and CPUs.

- Communications systems, including the normal rf and uhf communication equipment as well as ECM equipment, which require digital and analog signals to be transmitted.
- The instrumentation and control systems that are required for normal in-flight control of the aircraft by the pilot, such as heads-up display. Control systems also require both analog and digital signals to be transmitted.

THE EMP THREAT

It was observed in the early 1960's that a nuclear explosion can create a large electromagnetic pulse (EMP), and Fermi had noted the possibility when nuclear weapons were first being developed. Various types of EMP have been identified and studied. The pulse characteristics depend greatly on a number of parameters, including the burst location and the position of the observer, the range of which is indicated by the use of such terms as high-altitude EMP, ground-burst EMP, source region EMP, and system-generated EMP. EMP is generated from the X rays and gamma rays from a nuclear burst which create moving electrons and ions. These moving charged particles generate spatial- and time-varying current densities which in turn produce the electric and magnetic fields of an EMP.

A nuclear burst at an altitude of 50 km or greater creates numerous gamma rays which interact with the earth's atmosphere and produce radially moving electrons by the Compton effect. These radially directed electrons are turned by the earth's magnetic field, creating a transverse current density. It can be shown that this transverse current density produces a fast and intense radiated electromagnetic pulse over a large area which is within the line of sight of the nuclear burst. Remote locations will experience the radiated plane wave of the EMP threat, even though far outside the range of other nuclear weapon effects. A time waveform often used to approximate the high-altitude EMP is shown in figure 2. Its Fourier transform is shown in figure 3. The general equation for the time waveform is presented in equation (1). The Fourier transform functions are presented in equations (2-4). Detailed EMP waveform calculations are usually classified and are system- and scenario-dependent. These waveforms will serve for discussion purposes in this report since it deals with generalized system responses.

$$E(t) = E_0 k [-\exp(\alpha t) + \exp(-\beta t)]$$

$$E_0 = \text{maximum electric free field} = 5 \times 10^4 \text{ V/m} \quad (1)$$

$$\alpha = 4.76 \times 10^8$$

$$\beta = 4 \times 10^6$$

$$k = 1.05$$

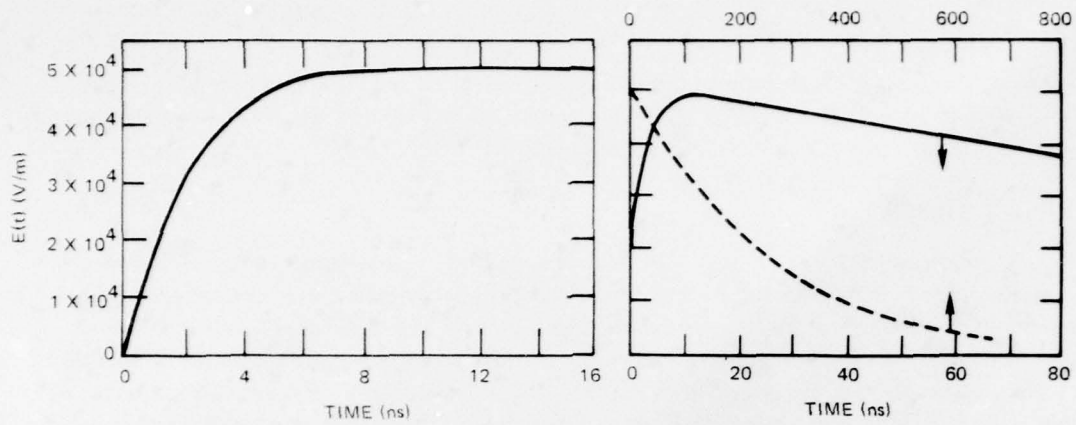


Figure 2. EM free-field pulse.

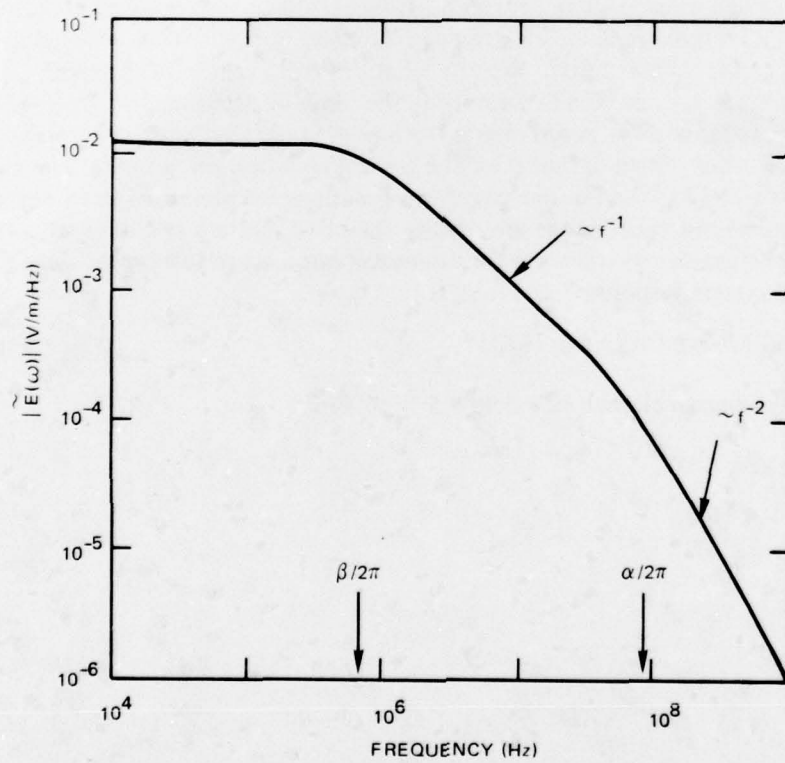


Figure 3. EMP frequency content (magnitude of Fourier transform).

Let $\tilde{E}(\omega)$ be the Fourier transform of $E(t)$.

$$\tilde{E}(\omega) = E_0 k \frac{\alpha - \beta}{(j\omega + \alpha)(j\omega + \beta)} \quad (2)$$

or

$$\tilde{E}(\omega) = E_0 k \frac{\alpha - \beta}{[(\omega^2 + \alpha^2)(\omega^2 + \beta^2)]^{1/2}} \quad \text{magnitude} \quad (3)$$

$$\arg [\tilde{E}(\omega)] = -\arctan \frac{\omega}{\alpha} - \arctan \frac{\omega}{\beta} \quad \text{phase} \quad (4)$$

$$\omega = 2\pi f \quad f = \text{frequency in Hz}$$

ELECTROMAGNETIC COUPLING IN AIRBORNE SYSTEMS

It is difficult to determine the potential vulnerability of fiber optic or any other electronic components in an incident EMP environment. This is because of the complex interactions of the electromagnetic coupling of a broadband signal to a system with many conductors. Airborne platforms consist of many signal and power cables which act as antennas for incident EMP signal pickup. In many cases, however, the receiver (ie, internal electronics) is detached from the antenna. For example, the "antenna" may be a shield designed to minimize any unwanted EM coupling to electronics (eg, an rf-shielded box often used to house electronics). Because no shield is perfect, however, some of the EM energy picked up by the system antenna will reach the electronics receiver. Determining just how much EM energy or signal reaches the electronics is the fundamental problem of EMP coupling.

Although specific details of aircraft design can vary substantially, a greatly simplified diagram indicating many typical electromagnetic features of an aircraft is shown in figure 4. Most aircraft have a conducting outer skin* which serves both as an antenna for picking up incident EM fields and as an inadvertent shield for internal electronics. This "shield" is rather leaky, however, with both deliberate EM penetrations (eg, radar and communication antennas) and inadvertent apertures (windows, doors, etc). Various avionics and communication equipments are located inside the aircraft. The electronics packages are connected by signal lines and power distribution system (which is often powered by generators attached to the aircraft engines).

Note that this system of conductors which make up the electromagnetic features of an aircraft can be quite complex. For example, an aircraft may have 10 or more deliberate antennas, hundreds of electronics boxes, and thousands of individual pins and connecting cables. Furthermore, the exact configuration of conductors (which is needed for EMP coupling analysis) may be poorly documented or unknown.

*Newer designs may have large sections of the outer skin made from lightweight composite materials which are dielectrics, thus providing little shielding.

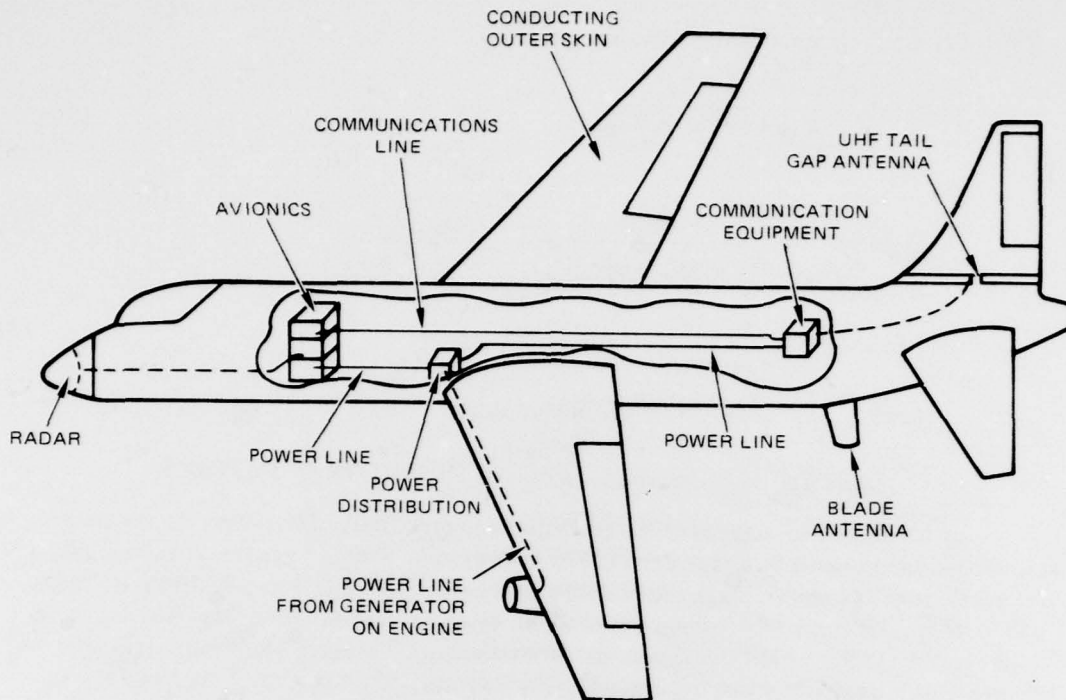


Figure 4. Simplified electromagnetic features of an aircraft.

For conceptual purposes, penetrations in this outer shield are often ignored in trying to calculate electromagnetic coupling to the outside of the aircraft. When the aircraft is present, the total EM fields near the outside are a combination of the incident EMP fields and the scattered fields that result from the skin currents and charge densities induced on the conducting skin.

The amount of EM leakage through various penetrations depends upon the types of penetration and the total fields near the m.

Similarly, internal EM fields will depend not only on the sources (ie, penetrations) but also on the internal electromagnetic configuration. The inside of an aircraft will typically contain a number of electronic boxes connected by signal cables and power lines. Box positions and cable routing are important in determining the amount of EM pickup. Boxes and cables may be shielded, providing a second layer of protection against the EMP threat.

Fiber optic systems are most likely to be used to replace conducting wire transmission systems. Coupling to a simplistic cable-box system is estimated in appendix A, and it is shown that replacing long conducting cables with fiber optic links can greatly reduce the effective volume over which electromagnetic energy is collected. To illustrate the magnitude of the problem, figures 5 and 6 display graphs of the equation for the electrical power per metre of cable coupled into a cable 5.06 cm in diameter, the center of which is located 2.54 cm off the ground plane, and which is exposed to the incident EM pulse of figure 2. This configuration is applicable to an aircraft which may have a cable bundle — strapped to the bulkheads and floors with plastic tie wraps — in which the outer jacket insulates the overall cable shield from the aircraft structure. Also shown in these figures is the free-field power as a function of time. The free-field power is derived by taking the square of the free field and dividing it by the impedance of space,

$$P_E = \frac{E(t)^2}{Z_0} \quad (5)$$

where $Z_0 = 377$ ohms. The important feature in figure 5 is that the coupled power peaks much faster than the incident pulse, then decays to zero and again increases after the peak of the incident pulse. This is because the coupled power is a function of the derivative of the square of the incident EMP electrical field.

A flowchart outlining various phases of the EMP coupling process is shown in figure 7. As indicated in this chart, the electromagnetic energy of the incident EMP waveform must follow a rather complex path before it reaches the individual circuits and devices where burnout or upset may occur. Note that the amount of energy which reaches a given device depends upon numerous system details including aircraft orientation, types of penetrations, cable configurations and shielding, and specific circuit design. Various features of this flowchart are also illustrated in figure 8.

The first step of the coupling process is the creation of induced skin currents and charge densities on the external conducting skin of the aircraft. The magnitude of the induced currents depends upon the orientation of the aircraft relative to the direction of propagation of the incident EMP planewave. Typical peak skin current densities may be roughly 10 times the peak incident magnetic field (ie, peak skin current densities of about 1000 A/m) at the resonant frequencies of the aircraft structure. Note that aircraft resonant frequencies correspond to aircraft dimensions, with typical values being in the range of 1 to 10 MHz. Skin current time histories are roughly approximated by damped sine waves; thus, even at the first step in the coupling process, the EM response no longer looks much like the incident EMP waveform.

The external surface current and charge densities just discussed are representative of the total magnetic and electric fields created outside the aircraft when it is exposed to an incident EMP. These fields can then leak through the outer skin via its numerous penetrations, either deliberate or inadvertent. Several such penetrations are illustrated in figure 9. Deliberate penetrations include antennas and radars, while there are numerous possible inadvertent penetrations including doors, windows, bomb bays, and other apertures. Examples of less obvious penetrations are hydraulic lines attached to control surfaces and generator pickup through engine air intakes.

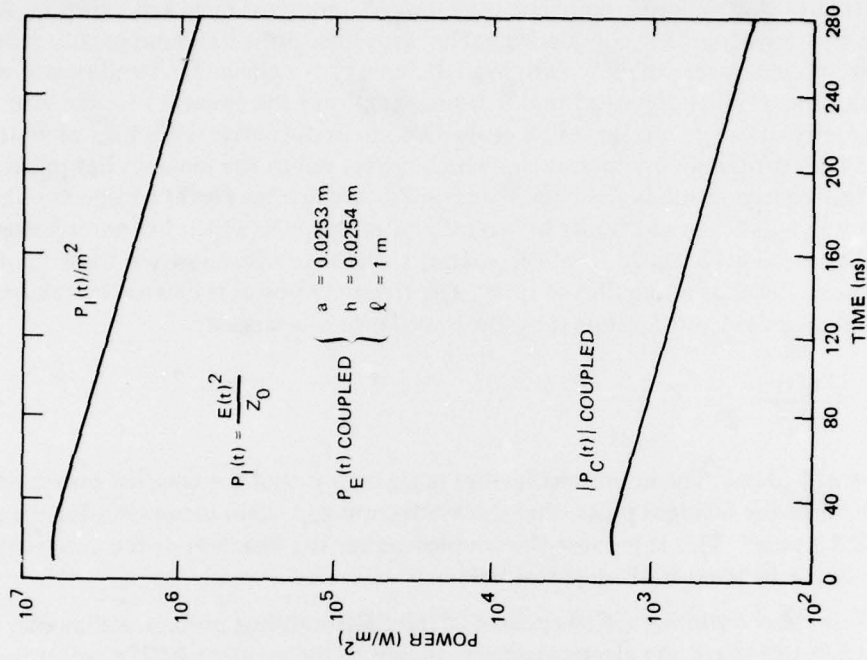


Figure 5. Free-field power per square metre of the incident EM pulse at maximum possible coupled power per metre of cable as a function of time for times less than 12 ns.

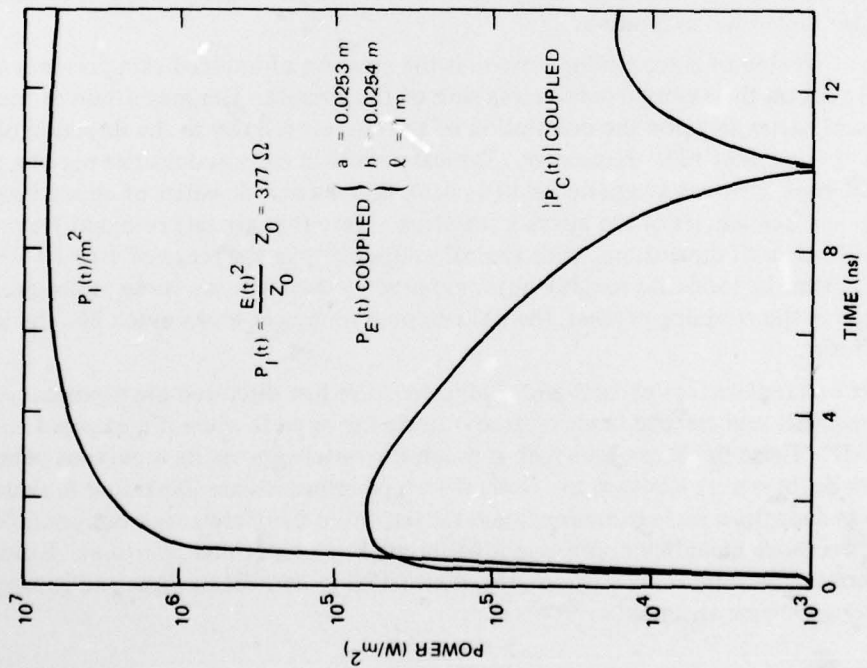


Figure 6. Free-field power per square metre of the incident EM pulse at maximum possible coupled power per metre of cable as a function of time for times greater than 12 ns.

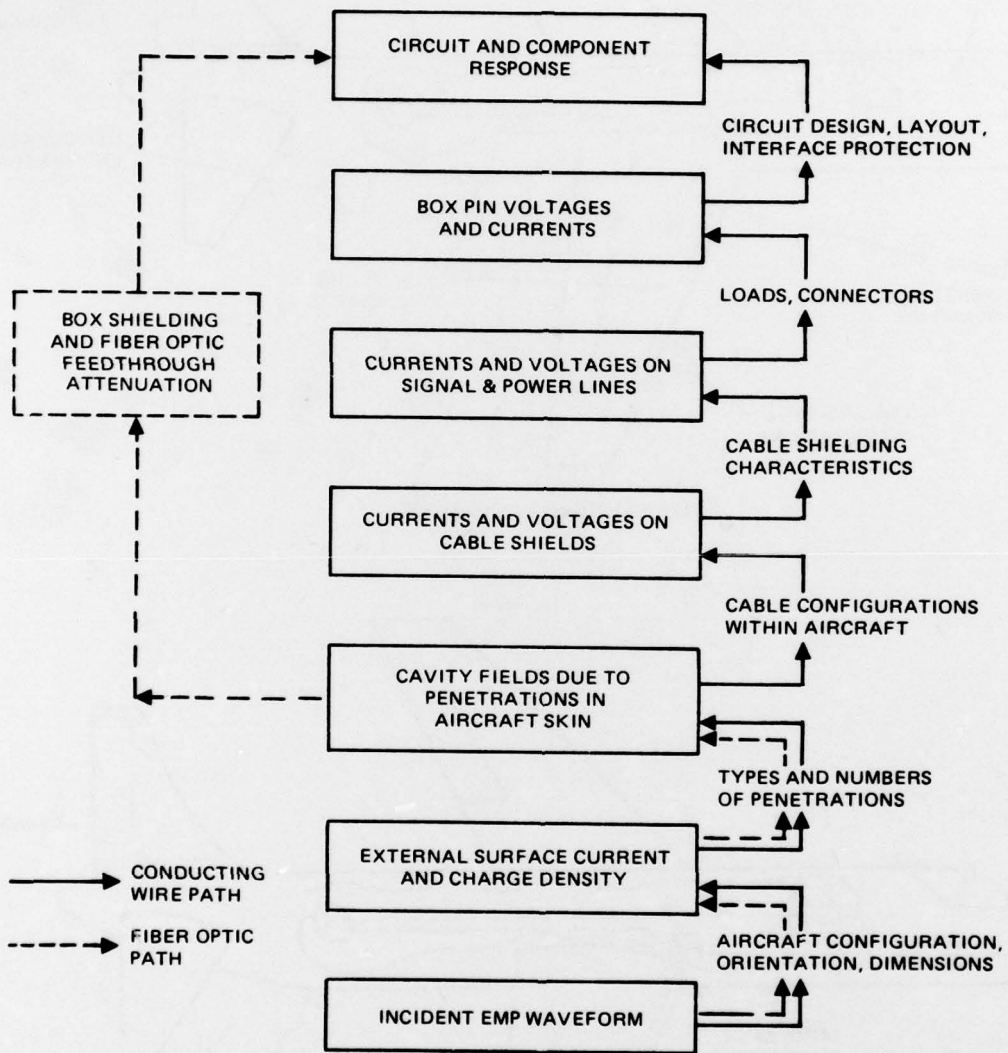


Figure 7. Flowchart of EMP coupling path.

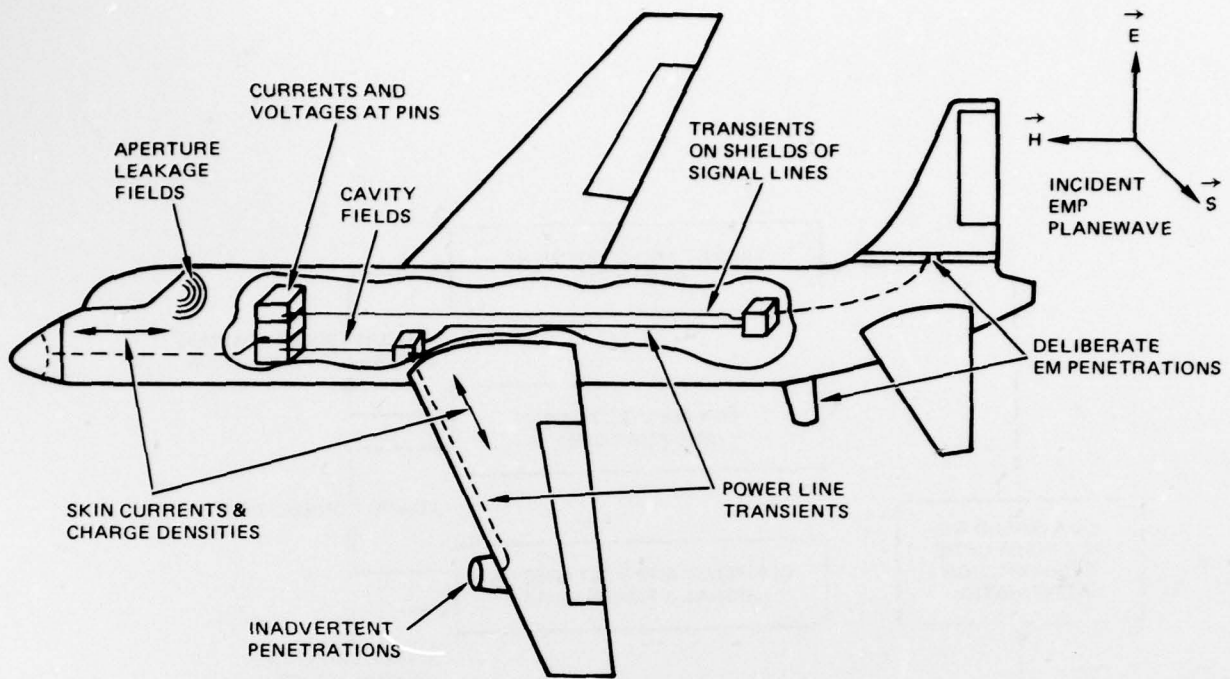


Figure 8. EMP coupling features.

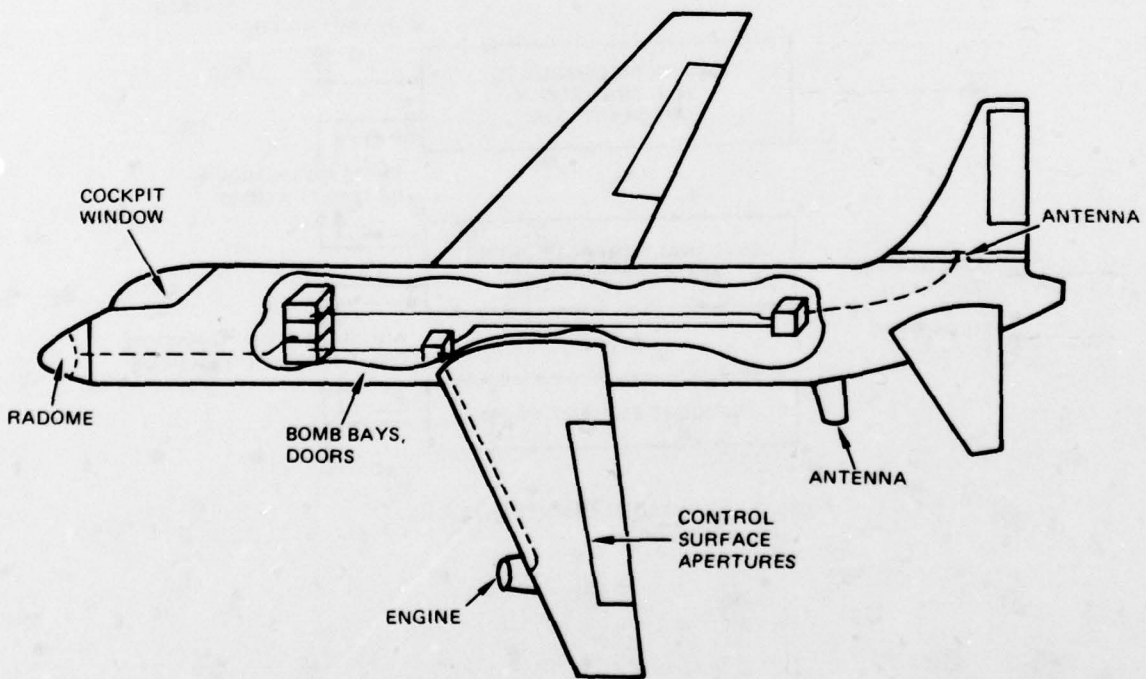


Figure 9. Points of entry for EMP energy.

The amount of EM leakage through the various penetrations depends on the type of penetration and the total fields near the penetration. Some penetrations are more sensitive to the local electric field, others to magnetic fields. Also, at some locations on the exterior, total electric fields will be large and magnetic fields small, while the opposite will be true elsewhere.

Internal EM fields will depend not only on the sources (ie, the penetrations) but also on the internal electromagnetic configuration. The position of electronics boxes and routing of cables will be important in determining the amount of EM pickup. Boxes and cables may also be shielded, providing a second layer of protection.

In conducting wire systems, the conducting wire itself is a major collector of EM energy (see appendix A). Conducting cables can thus channel energy from large volumes directly to electronics boxes. The next step in the coupling path flowchart for conducting links is, thus, the resulting currents and voltages on cable shields. As an example, currents of about 100 A/m may flow on a cable trough used as a bulk cable shield.

Note that figure 7 indicates that the coupling path for fiber optic links changes from that of a conducting link at this point. Optical fibers are insensitive to EM fields, although the associated transmitters and receivers are not. The fiber optic coupling path thus goes directly from cavity fields to EM leakage into shielded boxes, either through the box wall or through fiber feedthroughs (see appendixes B and C).

For conducting wire systems, however, experience indicates that the conducting links are often not only the dominant "antennas" for collecting EM energy but also the primary source of EM leakage. Cable (and connector) shielding characteristics then determine just what currents and voltages are induced on signal and power lines.

These cable transients produce currents and voltages at the various pins of an electronics box. The magnitude of these pin signals depends on the impedance seen at the pins. Note that the pins are directly connected to electronic circuits inside the box, although perhaps through filters or protective devices. Aircraft tests in EMP simulators have indicated that currents greater than 1 ampere may be induced on about 20% of the pins measured.

The final step in the coupling process for either fiber optic or conducting paths is at the circuit and component response level. If either upset or burnout can occur, EMP poses a significant threat to system performance.

One point to note from this brief discussion of EMP coupling to aircraft is that the coupling path for fiber optic systems is simpler than that for conducting links. Because the fiber links can be ignored, not only is the conceptual process simplified but also physical hardening techniques may be more easily implemented (ie, simplification makes errors less probable).

Fiber optic systems also tend to avoid the concentration of EM energy that is possible with conducting cables by reducing the effective antenna size; fibers are also advantageous in that they do not provide a direct conducting penetration through the walls of the electronics box.

Although the use of fiber optic links may reduce the need for conducting cables between boxes, the requirement for well shielded electronics boxes is at least as great for optical links as for conducting links. The reason, of course, is that optical signals are converted to or from electrical signals at the receiver or transmitter. The inside of a box is thus primarily electronics, which is susceptible to upset or burnout from EM fields. Also, fiber

optic receivers, in particular, are designed to operate at very low optical power levels. This tends to imply that they may also be sensitive to very small EM power levels.

In any case, it is clear that, for the various types of electronics associated with fiber optic systems, the primary protection is the EM shielding provided by the walls of the electronics box. As previously indicated, the electromagnetic environment seen by the box is not simply relatable to the incident EMP environment but will actually depend upon the external response of the entire system and the subsequent EM coupling down to the box level. The fiber optic system designer, however, will seldom have an overall view of system coupling, and he should thus design his box shielding to be relatively insensitive to such details.

An example of aircraft EMP coupling that includes all the various steps shown in figure 7 would be too lengthy and complicated for this report. A simplistic example of coupling to a cable which connects two electronics boxes is given in appendix A, however. This example ignores the exterior resonant skin currents and numerous penetrations of any real aircraft. Instead, the EM pulse is assumed to be directly incident upon two boxes sitting on a conducting ground plane and connected by a cable. Although unrealistic, this simple example does illustrate that only part of the incident electromagnetic energy is absorbed by any system (the rest is reflected).

The Fourier transforms for both the incident free-field power and energy are given in figure 10 (see equation (6)). Note that in this figure most of the incident energy is located

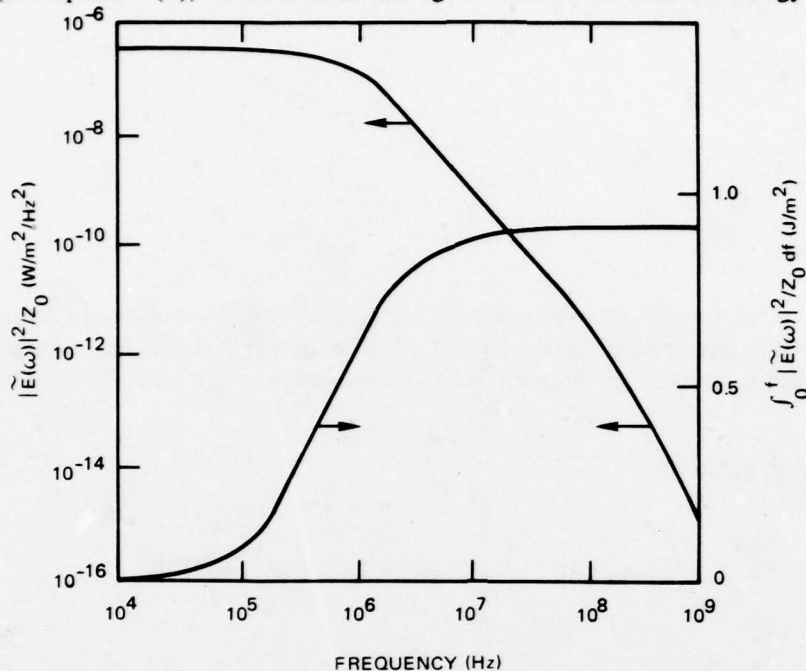


Figure 10. EMP power and cumulative energy per unit area.

$$\int_0^f \frac{|E(\omega)|^2}{Z_0} df = \frac{E_0^2 k^2}{\pi Z_0} \frac{(\alpha - \beta)^2}{\alpha^2 - \beta^2} \left\{ \frac{1}{\beta} \tan^{-1} \left(\frac{\omega}{\beta} \right) - \frac{1}{\alpha} \tan^{-1} \left(\frac{\omega}{\alpha} \right) \right\} \quad (6)$$

within the 10^5 - 10^7 -Hz frequency spectrum. This is the frequency range in which a significant number of military systems transmit data. It can also be seen that the total energy per m^2 incident upon the system is on the order of $0.9 J/m^2$; however, as seen in figure 11, the peak energy, W_C , coupled to the particular cable is 5×10^{-4} joule per metre of cable. The equation used for this graph of the coupled energy, W_C , was derived by taking the integral with respect to time of the expression for the maximum possible coupled power, as presented in appendix A. That is,

$$W_C = \int P_C(t) dt \quad (7)$$

Using this equation for P_C results in

$$W_C = h^2 \ell \frac{\pi \epsilon_0}{\cosh^{-1} \left(\frac{h}{a} \right)} \int \frac{d[E(t)^2]}{dt} = h^2 \ell \frac{\pi \epsilon_0}{\cosh^{-1} \left(\frac{h}{a} \right)} E(t)^2 \quad (8)$$

The coupled energy is then directly proportional to the length ℓ of the cable and the square of the incident field $E(t)$, or

$$W_C = \ell D E(t)^2 \quad (9)$$

where

$$D = \frac{h^2 \pi \epsilon_0}{\cosh^{-1} \left(\frac{h}{a} \right)}$$

Graphs of the free-field energy per unit area that is incident upon the system as a function of time are presented in figures 11 and 12. This energy is derived by taking the integral with respect to time of the equation for the free-field power as presented in figure 5.

$$\begin{aligned} W_I(t) &= \int P_I(t) dt \\ &= \frac{(E_0 k)^2}{Z_0} \int [\exp(-2\alpha t) - 2 \exp(-\alpha + \beta)t + \exp(-2\beta t)] dt \\ &= \frac{(E_0 k)^2}{Z_0} \left[(1/2 \alpha) \exp(-2\alpha t) - \frac{2}{\alpha + \beta} \exp(-\alpha + \beta)t + \frac{1}{2\beta} \exp(-2\beta t) \right] \quad (10) \end{aligned}$$

This could be reduced by picking the height above the ground plane so as to minimize the coupling into the cable. Assuming that this cable is a shielded cable or run in a conduit, the energy coupled into the inner conductors would be reduced by an amount equal to the shielding effectiveness (S_E) of the particular cable or conduit (see appendix B).

Fiber optic systems tend to avoid the concentration of EM energy that is possible with conducting cables by reducing the effective antenna size; fibers are also advantageous in that they do not provide a direct conducting penetration through the walls of the electronic box.

Although the use of fiber optic links may reduce the need for conducting cables between boxes, the requirement for well shielded electronic boxes is at least as great for optical links as for conducting wire links. The reason, of course, is that optical signals are converted to or from electrical signals at the receiver or transmitter. Inside the box are primarily electronics, which are susceptible to upset or burnout from EM fields. Fiber optic receivers are designed to operate at very low optical power levels. This implies that they may be sensitive to the same EM power levels.

For the various types of electronics associated with fiber optic systems, the primary protection is the EM shielding provided by the walls of the electronics box. As previously indicated, the electromagnetic environment seen by the box is not simply relatable to the incident EMP environment. It will actually depend upon the external response of the entire system and the subsequent EM coupling down to the box level. The fiber optic system designer, however, will seldom have an overall view of system coupling and should therefore design the box shielding to be relatively insensitive to such details.

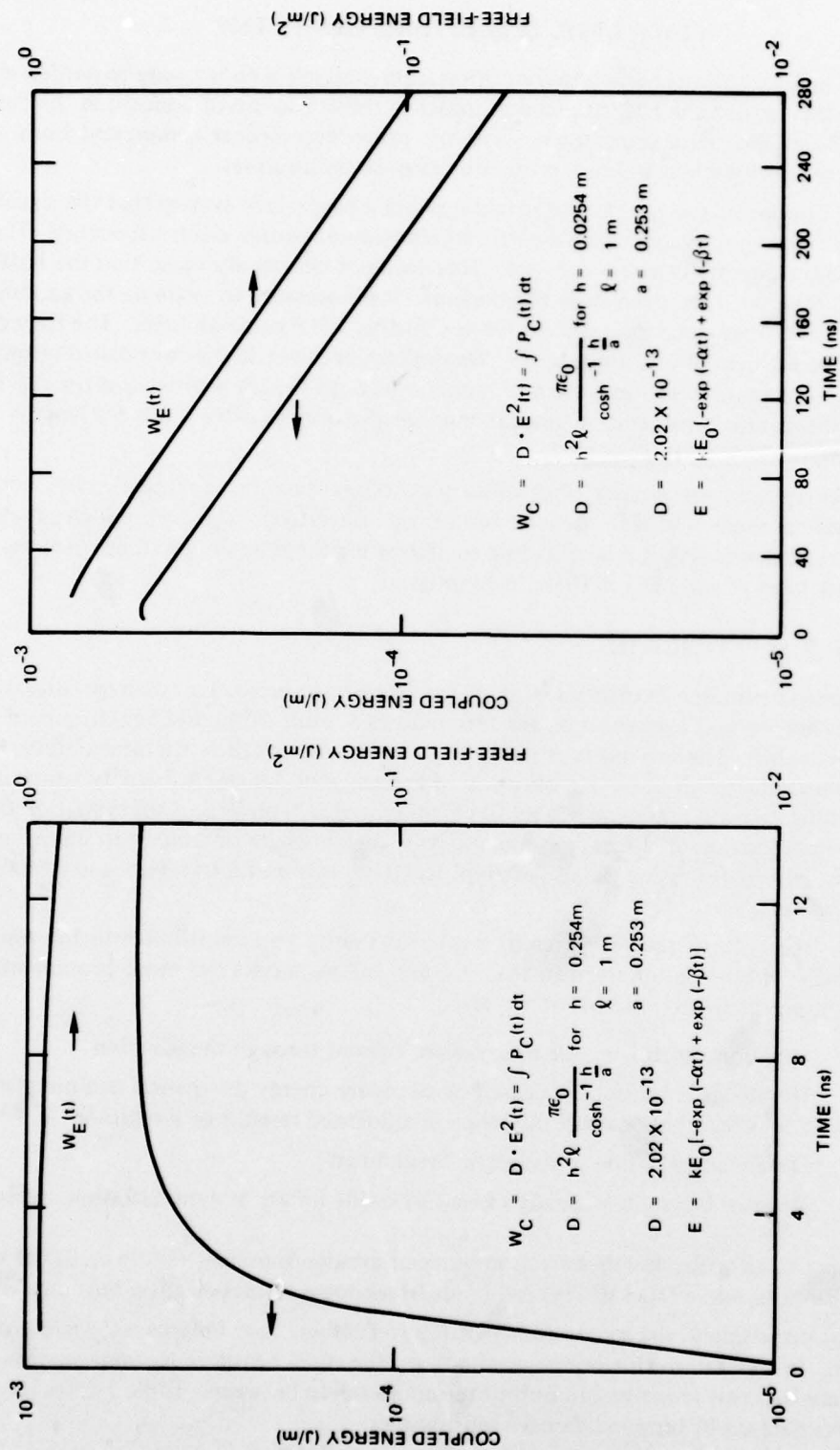


Figure 11. Coupled energy per metre of cable and free-field history for time less than 14 ns.

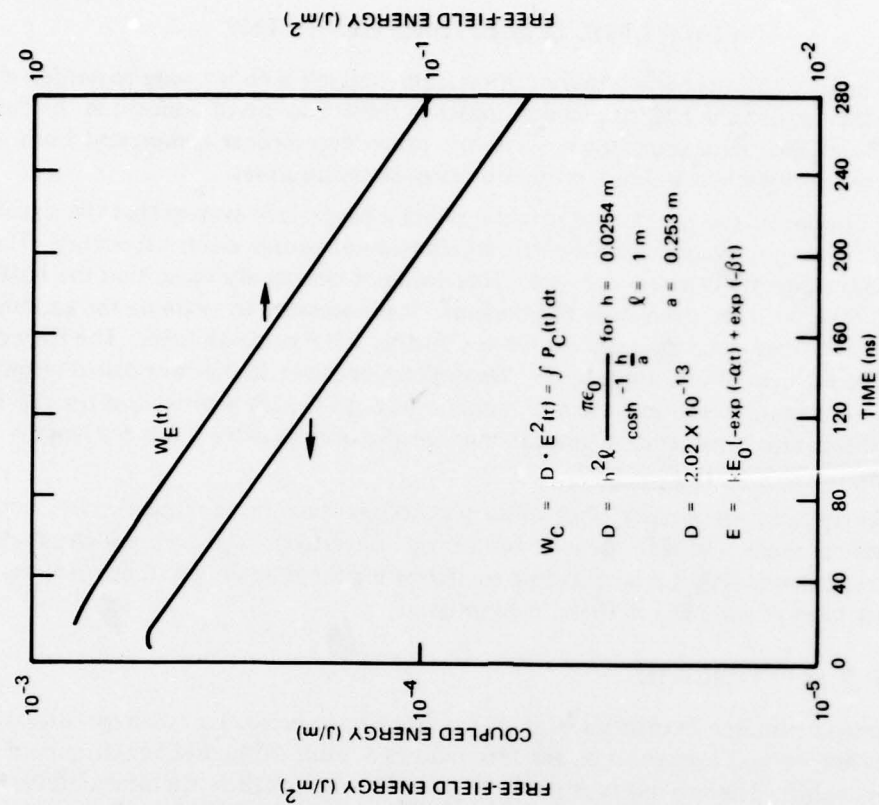


Figure 12. Coupled energy per metre of cable and free-field history for time less than 14 ns.

FIBER OPTIC SUSCEPTIBILITIES TO EMP

The major concerns of the fiber optics system designer who is trying to harden an airborne system against the EMP threat are similar to those that are of concern in the design of any EMP-hardened data transmission system: protection against component burnout and, if system specifications require, protection against circuit upset.

The fiber optic system has the advantage over a hard-wired system that the signal path for the fiber optic system is a dielectric which will not couple electrical energy. Thus, the signal path susceptibilities are reduced. This does not necessarily mean that the EMP threats have then been removed from the systems. It is necessary to examine the various constituents of a fiber optic data system for any further EMP vulnerabilities. The fiber optic system will be segmented into three parts: transmitter, receiver, and power distribution system. The power distribution system is common to both the transmitter and the receiver but warrants separate consideration since it contains the only possible paths for lengthy hard-wire interconnects.

Since systems employing fiber optic technology have been implemented, and probably will be implemented in the near future, via integrated circuit technologies that are already well developed, it is worthwhile to digress for the moment to summarize the burnout and upset phenomena in these technologies.

BURNOUT SUSCEPTIBILITIES

The susceptibility level of integrated circuits (ICs) to permanent damage caused by the currents and voltage impressed on the terminals as a result of the EMP environment varies considerably. The variability is partly the consequence of the structural variety found in these semiconductor devices. An overview of the range of damage sensitivity which can be expected from several popular IC families is presented in figure 13. Determination of the range of thresholds expected for a particular device type must be obtained through empirical data, but before discussing the use of empirical data, it is useful to review some models of the damage process.

The existence of several different modes of failure also contributes to the range in the damage thresholds observed in ICs. Certain failure modes are more prominently observed during electrical pulse overstress tests:

1. Junction shorting – due to excessive current through the junction
2. Metalization burnout – caused by excessive energy dissipation in a metalization stripe, or by heat generated beneath the stripe in a diffused resistor or junction
3. Oxide failure – due to dielectric breakdown
4. Resistor burnout – usually caused by oxide failure at a metalization crossover

Junction shorting and metalization burnout are the dominant failure modes observed in bipolar circuits, while MOS ICs exhibit oxide breakdown or metalization burnout.

Not surprisingly, the susceptibility of ICs to EMP-induced failures is device-terminal-dependent. In general, device input terminals are the most sensitive to damage. Power terminals are the least sensitive and output terminals fall in between. Table 1 shows some comparative data on IC terminal damage sensitivities.

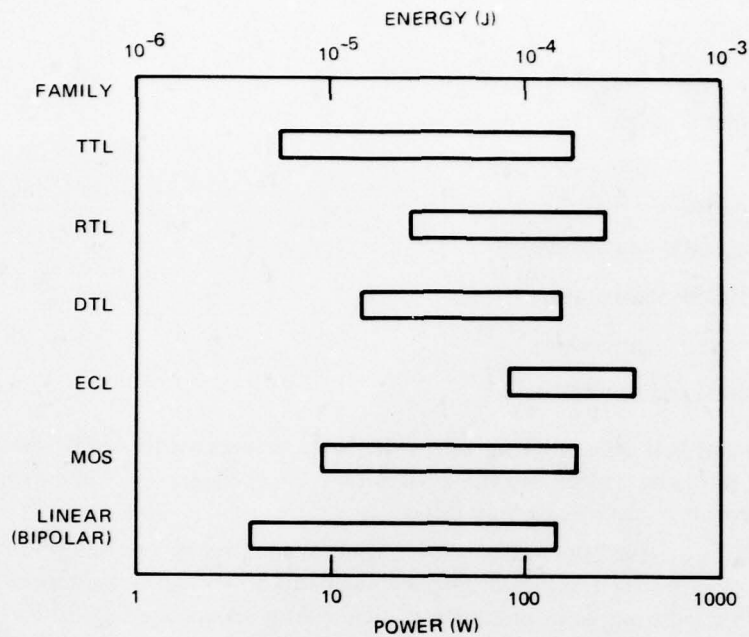


Figure 13. Range of observed input terminal failure thresholds for 1-μs pulse.

Table 1. IC terminal damage thresholds for 1-μs pulse*.

IC Family	Terminal	Damage Threshold (μJ)
TTL	Input	29
	Output	77
MOS	Input	43
	Output	116
	Power	190
Linear	Input	84
	Output	267

*From ref 5.

In 1968 Wunsch and Bell (ref 1) published their now well known equation relating power dissipated in a semiconductor junction to the time to failure:

$$\frac{P}{A} = \sqrt{\pi \kappa \rho C_p} (T_m - T_i) t^{-1/2} \quad (11)$$

1. DC Wunsch and RR Bell, Determination of Threshold Failure Levels of Semiconductor Diodes and transistors due to Pulsed Voltages, IEEE Trans Nucl Sci NS-15, no 6, December 1970.

where

- P = power (dissipated in junction)
- A = junction area
- κ = thermal conductivity
- ρ = density
- C_p = specific heat of silicon
- T_m = failure temperature
- T_i = initial temperature
- t = time (pulse width)

Wunsch and Bell were working with voltage stress pulse widths of between 100 ns and 20 μ s. For the pulse widths and the devices they checked, the $t^{-1/2}$ time dependence was found to provide a good fit to their data.

In 1970, Tasca (ref 2) provided a more general equation for pulsed-power failure in a semiconductor junction. Considering second breakdown as the damage mode and imposing certain conditions to estimate the critical energy to initiate second breakdown, Tasca arrived at

$$E_c = \left(\frac{4}{3} \pi a^3 \rho C + 4\pi a^2 \sqrt{\rho C \kappa t} + \frac{8}{3} \pi a \kappa t \right) (T_C - T_A) \quad (12)$$

where

- E_c = energy to achieve temperature rise $T_C - T_A$
- T_C = current construction site temperature
- T_A = ambient temperature
- a = radius of spherical defect region
- t = time
- κ = thermal conductivity
- ρ = density
- C = specific heat

The conditions which Tasca assumed were:

1. Second breakdown occurs at a single current construction site in the junction; the site is the weak link in the junction thermal system.
2. The weak link site is of such severity that essentially all the junction current is passed through it.
3. The severity of the site is such that it precludes a significant amount of heat being dissipated to it from the surrounding medium (bulk material) and only dissipates heat to the medium.

2. DM Tasca, Pulsed Power Failure Modes in Semiconductors, IEEE Trans Nucl Sci NS-15, no 6, December 1970

4. The site can be approximated by a spherical geometry, with radius a constant until second breakdown occurs.

5. Heat is produced at a constant rate per unit time per unit volume in the spherical deflection region.

In the Tasca model, the relationship between E_C (energy required to reach the critical temperature to initiate thermal second breakdown) and pulse width depends on the time regime of the pulse width. There is first a constant energy condition for short pulse widths, then a one-half power time dependence for longer pulse widths, and a linear time dependence at thermal equilibrium. Empirical results have shown that E_C is independent of pulse width up to 10-100 ns, with the one-half power dependence holding up to about 10-20 μ s.

The thermal models for describing pulsed-power failure of semiconductor junctions have been developed from data gathered on discrete semiconductor devices (transistors and diodes). While the primary failure mode for ICs is undoubtedly thermal also, extension of the discrete device models to ICs must be done with care. It is reported (ref 3) that for ICs the value of the exponent B in the equation

$$P_F = At^{-B} \quad (13)$$

for pulse widths of 0.1-10 μ s can range from 0.1 to 1.0.* In ICs, this range can be attributed to the many alternate current paths available for any given terminal, where the primary current path for failure does not carry the total current impressed on the terminal.

A failure mode which is occasionally observed in ICs is nonthermal in nature and is characterized by unpredictable, and significantly lower, energies than required for bulk damage at similar pulse widths (ref 4). The failure mechanism consists of a voltage-sensitive surface breakdown which results in a shunt leakage path around the junction. This failure mode is observed at narrow pulse widths and is characterized by a constant voltage and power as a function of pulse width, indicating that a voltage threshold has been reached.

Empirical damage data are often presented in terms of the damage constants for one of the above models to facilitate scaling from the simulation conditions to the pulse width of the anticipated threat. Given the statistical nature of the damage thresholds, a safety factor of at least 10 is recommended as a design margin for EMP-induced device burnout.

UPSETS

EMP-induced upsets in fiber optic data systems occur as a result of energy coupled into the system via complex system-independent paths or, for those systems that may be mounted on external surfaces or appendages, by direct interaction with the EMP environment. The susceptibility of the fiber optic system is the same to these signals as to other

*In fact, it seems that many discrete devices show a wide range in the value of B also (see ref 3, p 2456).

3. CR Jenkins and DL Durgin, EMP Susceptibility of Integrated Circuits, IEEE Trans Nucl Sci NS-33, no 6, December 1975

4. C Kleiner, J Nelson, F Vassallo, and E Heaton, Integrated Circuit Model Development for EMP, IEEE Trans Nucl Sci NS-21, no 6, December 1976

EM-coupled noise energies. These specifications are usually given in terms of noise margin and dc characteristics of the particular logic family. For the EMP-induced transients into the system, this is not a good measure of the upset levels for that particular logic family. A better measure of upset levels caused by these fast transients would be the amount of energy required within the coupled signal to cause an upset. An excellent article (ref 5) discusses the noise energy required to cause upsets in various semiconductor logic families and concludes that for the data lines the noise energy, E_N , may be given as

$$E_N = \frac{V_N \times (PW)}{R_0} \quad (14)$$

where

V_N = noise voltage amplitude required to cause a circuit malfunction

R_0 = line impedance

PW = noise pulse width

A plot of this equation shows that there is a minimum noise energy that will cause circuit malfunction.

For power leads, supplies and grounds, the ac noise voltage induced on these lines is more meaningful since the energy required to produce this voltage is highly dependent upon the power supply output impedance and the particular bypassing techniques that may be employed within the individual system boxes.

A summary of the minimum noise energies for data lines and the ac power supply noise voltages required to cause circuit upsets is given in table 2.

It should be pointed out that, with the exception of the HTL logic family, all the noise energy minimums are less than 10 nJ. Although some very important logic families are not included in this report (LPST², ST²L, and I²L), their noise immunities should be very close to this range (1-10 nJ) and would not be expected to exceed 10 nJ. Because of the current injection rails connected to the power supply in I²L technology, this technology may have better potential for ac power noise immunity than the other technologies, but most practical devices manufactured today have buffers to exit the chip which are T²L- or LPT²L-compatible. These buffers will probably have ac noise immunities similar to those of their parent logic families.

5. Alan Allen, Noise Immunity Comparison of CMOS Versus Popular Bipolar Logic Families, Motorola Application Note AN707 (1973)

Table 2. Noise immunity results.

Logic Family/ (Gate)	Power Supply (volts)	Typical Quiescent Delay Dissipation (mW)	Typical Propagation Delay (ns)		Typical Power Supply Line AC Noise Margin (volts)	Typical Ground Line AC Noise Margin (volts)	Low	High	Typical Noise Energy Minimum			
			t _{PHL}	t _{PLH}					ENL (nJ)	at PW (ns)	ENH (nJ)	at PW (ns)
DTL (MC849)	5	8	20	50	3.0	1.0	49	1.8k	1.4	45	0.4	40
TTL (MC7400)	5	10	8	12	3.0	1.0	30	140	1.7	20	1.0	25
HTL (MC672)	15	25	85	130	6.0	4.5	140	1.6k	60	125	5.0	145
CMOS (MC14011)	5	$25 \cdot 10^{-6}$	35	100	2.8	1.0	1.7k	4.8k	1.0	155	0.9	280
	10	$50 \cdot 10^{-6}$	20	35	5.7	4.3	670	1.5k	3.7	70	3.1	90
		$150 \cdot 10^{-6}$	8	15	8.5	6.4	460	1k	7.2	50	8.5	75

FIBER OPTIC TRANSMITTER SUSCEPTIBILITIES TO EMP

Fiber optics (FO) transmitters are similar to hard-wire transmitters used to drive 50- or 93-ohm coaxial or twisted shielded pair (TSP) data lines in that both buffer the relatively low-power data input signals to provide enough power to drive the data transmission path. A schematic diagram is shown in figure 14. For the digital case of a typical fiber optic digital transmitter, many of the components are the same; ie, T²L 50/93-ohm line drivers and hex buffers can be used to drive the optical power source (LEDs), and both types of transmitters should have similar vulnerability levels with respect to coupled energy. The hard-wired system must have an electrical path outside the box and will, therefore, be subject to large transients induced on these cables if their lengths are significant (see appendix A). If extra circuit protection has not been provided (ie, shielding, bandpass filters, or surge suppressors), these large transients will cause failures within the devices.

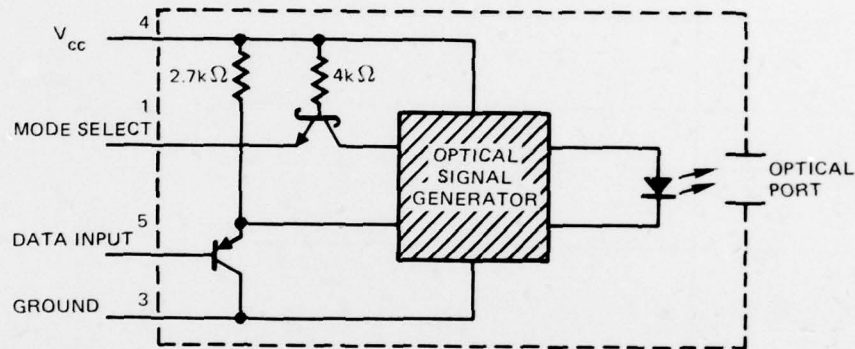


Figure 14. Schematic diagram of FO transmitter.

For T²L line drivers, the burnout threshold has been observed to be on the order of 100 μ J of electrical energy at the output pins (ref 6). This threshold is within the range of the burnout thresholds of the rest of the integrated circuit families listed previously in table 1.

In hard-wired systems that have moderate length ($l < 10$ m), obtaining enough shielding effectiveness to reduce the coupling below the output burnout thresholds of even the most sensitive logic families (~ 70 μ J) is relatively easy. However, for the hard-wired system, protection of the digital logic connected to the data lines in the cable against electrical upset will require that the coupled energy be reduced below the 1-nJ upset energy threshold. This requires an additional 50 dB of shielding and coupling loss. This is considerably harder to obtain since the majority of the energy spectrum of the EM pulse is within the digital bandpass. For this reason, EMP-hardened hard-wire systems usually employ a means of limiting this coupled energy.

6. JA Plumer, Lighting and Electrical Systems, Interface Technology Engineers Master 1978, p 188-192.

For FO data transmitters, the direct paths for coupling energy into the electronics via solid conductors are eliminated except for the power leads, which are covered in a subsequent section. This assumes, of course, that the electrical data input to the FO transmitter is not routed through long cables that exit the shielded enclosures containing the FO transmitter. The other paths for coupling energy into the FO transmitter are through the walls of the enclosure and through the deliberate penetrations in it. Assuming that in a practical system the volume of the enclosure containing the FO transmitter is less than the effective volume of the cable (see appendix C), the shielding effectiveness requirements for the enclosure are not as great as for the cable. This does not imply that the systems designers can be careless in designing or selecting enclosures; good rf-tight enclosures should always be used in EMP environments. Penetration through the walls of the enclosure is a necessity for both hard-wired and FO data transmitters; therefore, sensitive components should not be located close to them. This is especially true of the inputs of the digital integrated circuits, since these are the most sensitive to upsets.

FIBER OPTIC RECEIVER SUSCEPTIBILITIES TO EMP

The optical power impinging upon an FO receiver is relatively small. Therefore, the sensitivity and gain must be greater than required by the hard-wired systems receiver. Because of these requirements, the FO receiver also becomes more susceptible to EM-produced interference, and care must be taken in its design to provide the necessary shielding around the receiver to allow it to operate in the EM environment encountered within the electronics package. A typical receiver design is shown in the schematic diagram of figure 15. In some systems, it is necessary to construct separate rf enclosures around the preamplifier for isolation from the rest of the electronics. The reason for this can be seen in figure 16. *This figure indicates the sensitivity requirements as a function of required data bandwidths for an optimized transimpedance preamplifier design that was developed and analyzed by Spectronics, Inc (ref 7).* In this design, the required optical power (P_n) at the photodetector for data bandwidths between 1 and 300 MHz is 1×10^{-9} to 5×10^{-7} watt, to establish a signal-to-noise ratio of unity (SNR = 1). For most systems, this is not an acceptable SNR. In analog systems, the bit error rate (BER) is dependent upon the SNR: the larger the SNR, the smaller the BER. The attainable SNR for a particular FO system is dependent upon many factors in the design and is beyond the scope of this effort. Suffice it to say that, for digital data systems, the detection level is set so that at the minimum design SNR the BER requirements can be met. Some systems do incorporate automatic gain and/or detection-level correction circuits which increase the dynamic range of the receiver. However, as far as single-event upsets are concerned, worst-case analysis should be done at the minimum SNR and most sensitive gain.

It should be pointed out that SNR is not the only design parameter that should be considered in determining receiver vulnerability to upsets. Equally important are the magnitude of the received data signal and the sensitivity of the receiver. For nonoptimally designed receivers, there exist three ways in which to increase the SNR:

7. JR Baird, Optoelectric Aspects of Avionic Systems II, AFAL-TR-45, May 1975

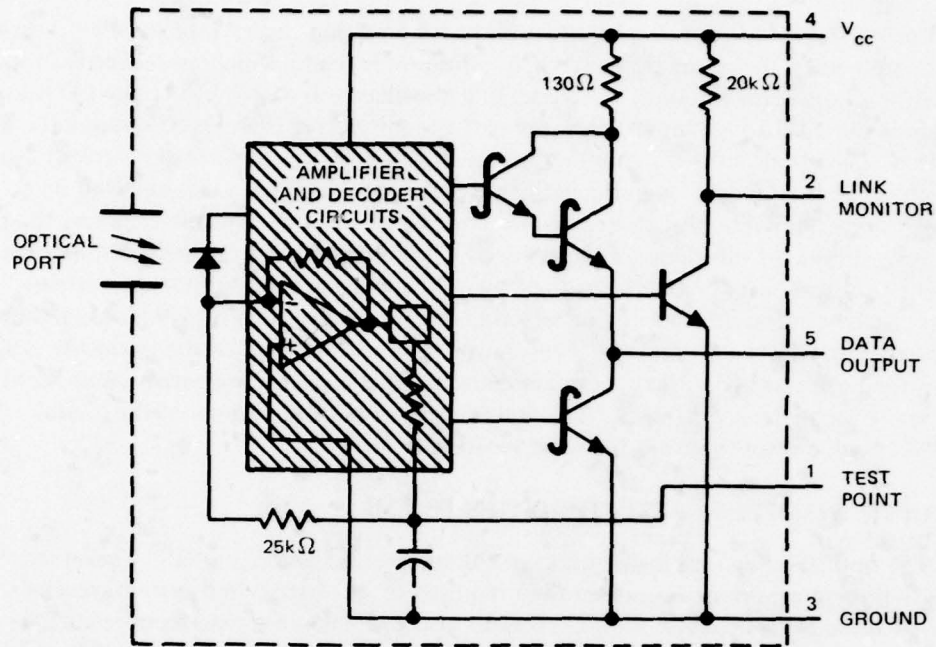


Figure 15. Schematic diagram of FO receiver.

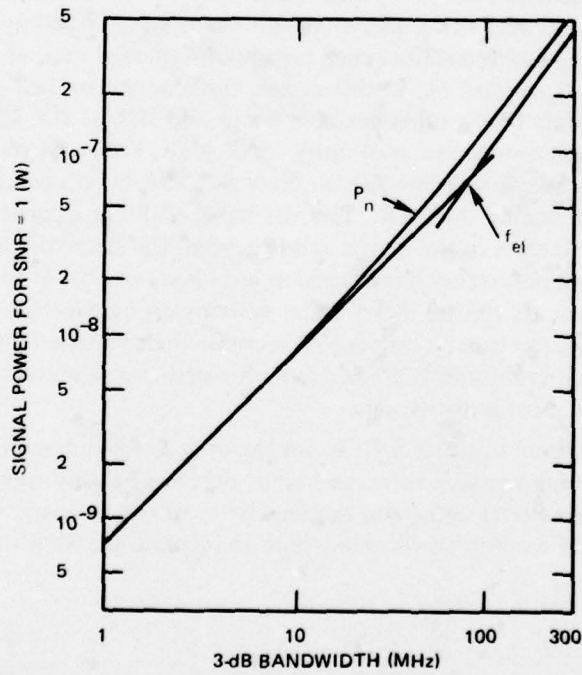


Figure 16. Photodiode/preamp noise characteristics (ref 7).

- Increase the received optical signal power
- Reduce the bandwidth of the system
- Reduce the receiver noise equivalent power (NEP) by redesign or selection of low-noise components

Of these, only the first two may contribute to reducing the receiver vulnerability to EMP-induced upsets.

The effect of the first is obvious: the more signal available at the receiver, the more noise required to overcome it. In the second method, the effect is a little more subtle. Receivers are designed to amplify signals within a certain bandwidth. For noise impinging upon it outside this bandwidth, the susceptibility of the receiver will depend upon the particular design. Usually the narrower the bandwidth and the faster it rolls off (steep skirts), the less susceptible the receiver will be to this out-of-band noise. As pointed out in figure 10, the majority of the energy associated with this typical EMP pulse is situated in the 1-10-MHz spectrum. It would then be advantageous to have the receiver operate outside this frequency range. For most data (except very low bandwidth, <100 kHz), this would mean modulating the data onto a carrier that is located above this frequency spectrum. Note that this is the case for the typical EM pulse under consideration here but may not be valid for other environments.

If the FO receiver is to operate baseband (without being modulated to a higher frequency), it should be designed to have as narrow a bandpass as possible. However, the designer is faced with the problem that a minimum bandwidth is required to pass the signal. In digital systems, this minimum bandpass will be dependent upon the encoding method chosen to transmit the signal. In selecting the encoding method, the system designer will have to make judgments as to tradeoffs involved in the various encoding techniques for his particular system and environment.

The third method does contribute to increasing the receiver SNR by reducing the noise in the receiver and thus allowing smaller data signals to be detected – ie, greater sensitivity. However, this will not make the receiver less susceptible to noise generated within the bandpass.

These points apply to the design of data bus systems, in which a tradeoff with respect to system reliability vs received power is made between the two usually considered system configurations – daisy chain and multipoint mixers. Multipoint mixers (or star couplers) require more sensitive receivers to establish the required SNR because of the extra losses within the couplers. For a 32-port coupler, this results in at least a 15-dB theoretical loss in signal power plus the excess losses within the coupler. An additional 30 dB of shielding would be required to reduce the EMP-induced signal by an equivalent amount. If ample optical power design margin (>10-15 dB) cannot be attained in the "star coupled" configuration, it is recommended that the "daisy chain" configuration be employed in the implementation of those data bus systems in which EMP hardening is a prime consideration.

To estimate the magnitude of the shielding problem for a typical receiver, consider a digital system with a 10-Mbit/s data rate that uses Manchester encoding (biphase). The receiver must be designed for a bandpass of 18 MHz (ref 5). From figure 16, the required optical signal (P_n) for the receiver is 2×10^{-8} watt. If a peak power of 6×10^6 W/m² in

the incident free-field pulse (fig 5) is used as the maximum threat, the attenuation required to reduce the coupled EMP signal below the system noise level is then 144 dB. If a 10^{-9} BER (22-dB SNR) and a signal midpoint detection level are assumed, this requirement could be reduced to 137-dB attenuation.

This attenuation is attainable, but care must be exercised in selection of enclosures and placement of components. For example, consider the 50-mil FO cable connector that was analyzed in appendix B. This connector has 70 dB of EM attenuation, resulting in the equivalent of $\sim 2 \times 10^3 \text{ W/m}^2$ at the end of the connector. For a photodetector mounted by butting against the end of the connector, 2.4 mW of electrical power will be incident. It is possible that this energy can be totally coupled into the input of the preamplifier if the case of the detector is isolated and connected to the preamp. It is therefore recommended that, for those systems which employ fiber optic bundles, pigtails be used to place the detector physically far enough away from the aperture to allow for dissipation of the coupled energy by the time it reaches the detector (see appendix C).

As a result of the receiver sensitivity to small amounts of energy at its inputs, it is also susceptible to coupled signals via other paths such as the power supplies. The magnitude of this susceptibility is dependent upon the individual receiver design. For the receiver to be insensitive to signals picked up on or generated in the power supply distribution system, it should be designed to have a good power supply rejection ratio (PSRR). Even with a good PSRR, extra filtering must sometimes be employed in the power supply leads to the receiver portion of the circuitry to provide the necessary isolation from the rest of the power supply system.

Burnout thresholds for receivers should not be significantly different from those for transmitters. One exception to this may be in the very-high-frequency designs, $>300 \text{ MHz}$, in which very-high-speed transistors are used. These devices have very narrow base widths and high doping levels. They are susceptible to low base-emitter and base-collector reverse breakdown voltages and should therefore be protected against overstressing.

EMP CONSIDERATIONS RELATED TO THE POWER SUPPLY DISTRIBUTION SYSTEM FOR FIBER OPTIC SYSTEMS

In those systems that contain their own energy sources (batteries, motor generators, solar arrays) within the same shielded enclosures, fiber optics represents a means of reducing the effective coupling volume (appendix A). However, there still exist systems that require the power supply to be distributed via conductors. For these systems, the effective coupling volume from the power source has not been reduced, but a good measure of EMP hardening may still be obtained because filtering of the EMP-induced signals is easier at the lower frequencies (dc to a few hundred hertz) of the distributed power.

To protect digital FO transmitters against burnouts and upsets due to signals coupled via the power distribution system will not require any more protection than would be required for similar hard-wired transmitter modules. Receiver burnout thresholds should also be comparable to those of hard-wired receivers. However, as pointed out in a previous section, the receiver can be highly susceptible to upsets caused by transients on the power bus. For systems in which transient upsets cannot be tolerated, extra filtering may be required (above the added filtering required at the receiver anyway) to reduce the high-frequency transients generated on the power system conductors to a level that will not adversely affect the receiver.

The amount of extra filtering required will depend upon the individual receiver design, length of cable, attenuation efficiency at high frequencies of the normal power supply filters, and the amount of shielding incorporated in the interconnect cables. On this last point, it should be emphasized that it will be necessary to maintain the interconnect wiring within a shield or else ensure by some other means that the incident EMP field has been attenuated below a level that will couple significant energies into the conductors. Also, in cable bundles in which data wires would normally be routed within the same shielded cables as the power distribution wiring, replacing these data wires with FO cables may also remove some of the shielding to the power conductors and thus increase the EM-coupled signals into the power conductors.

EMP HARDENING TECHNIQUES

Electronic vulnerabilities to EMP are commonly categorized as burnout effects or upset phenomena. Burnout is primarily a function of electromagnetic energy delivered to device junctions, where deposited energy can cause permanent device damage. Upset, on the other hand, refers to a temporary or permanent malfunction in the operational functioning of an electronic system. If the system can quickly recover, a temporary upset may be acceptable. Permanent upset or burnout is almost never acceptable.

Hardening techniques can also be categorized along these lines. Burnout protection requires either some type of EM shielding to attenuate the incident energy or additional protection at the circuit level. Such shielding will also alleviate upset problems, but upset hardening can also be accomplished at the circuit level by building in upset-tolerant designs and automatic reset capabilities.

ELECTROMAGNETIC SHIELDING

The concept of electromagnetic shielding is based on the fact that the region inside a completely closed, perfectly conducting enclosure will be totally isolated from any external electromagnetic fields. Real materials are not perfectly conducting, however, and real enclosures are seldom completely closed. Electromagnetic fields will thus penetrate realistic shields, although the amount of penetration is a strong function of shield design and the frequency content of the external fields (ref 8,9).

There are two basic processes by which EM energy can penetrate a shield. The first is diffusion, which occurs because real conductors have finite, although large, conductivities. The second is leakage through holes or apertures in the shield. Such apertures may be deliberate, so that equipment on the inside of a shield can communicate with the outside, or accidental, due to access doors, hatches, or connectors improperly attached or closed.

The primary parameter for characterizing diffusion through a conductor is skin depth, δ , where

$$\delta = \frac{1}{\sqrt{\pi f \mu \sigma}}$$

8. Special Joint Issue on the Nuclear Electromagnetic Pulse, IEEE Trans Ant Prop AP-26, no 1, January 1978 [Also IEEE Trans EMC, EMC-20, no 1, February 1978]

9. CM Butler et al, Selected Topics in EMP Interaction, AFWL Interaction Notes, IN-339, August 1976

In this equation, f is frequency of the EM wave, μ is magnetic permeability, and σ is conductivity. The skin depth is the enfolding distance for attenuation of a plane wave incident upon a conducting planar surface. Thus, we should like the thickness of any EM shield to be many skin depths at all frequencies of interest. As a specific example, the skin depth in copper at a frequency of 1 MHz is about 5×10^{-3} cm.

Note that the skin depth increases as the frequency decreases. At static cases, however, a completely closed conductor will still do an excellent job of excluding electric fields. (The conductor acts as a Faraday cage, a concept familiar for electrostatic protection.) Low-frequency magnetic fields will, however, penetrate good conductors. If low-frequency magnetic fields are thought to be a problem, high-permeability materials (eg, mu-metal) are often used as shielding materials. It is apparent from the definition of skin depth that increasing μ will decrease δ .

In the majority of cases, EM diffusion through good conductors is not the limiting factor for determining shielding effectiveness. More often, the majority of EM energy leaking to the inside of a shield comes through various apertures, deliberate or inadvertent. Small apertures are often characterized in terms of their electric and magnetic polarizabilities. These geometrical factors must be combined with a knowledge of the external EM fields near the aperture to estimate the amount of energy that leaks inside. A description of the details of aperture coupling is beyond the scope of this document, but the interested reader can examine several publications on the subject (ref 8,9).

The designer will often see EM shielding quantified (ref 9) in terms of the shielding effectiveness parameter, S (see appendix B for a more detailed discussion), where

$$S = 20 \log_{10}[\eta] \text{ dB} \quad (15)$$

and

$$\eta = \frac{\text{amplitude of electric (or magnetic) field inside shield}}{\text{amplitude of electric (or magnetic) field incident on shield}}$$

Although a useful parameter, the shielding effectiveness is not a unique function that totally describes a shield. It is uniquely defined for plane waves incident on an infinite planar conductor, where it depends only on the frequency of the incident wave. For finite conductors, or those with apertures, it is also a function of the location at which it is being determined or the method by which it is being calculated or measured. These limitations should be considered when this parameter is used.

As mentioned previously, the fiber optics designer will be most interested in shielding at the electronics box level. Shielding effectiveness, as calculated by the methods presented in appendix B, would imply to the uninformed that a metallic box constructed from a sheet of one of these materials would have increasing shielding effectiveness as the frequency is increased. However, this is not the case in a practical situation. In fact, the opposite is true, as can be seen in figure 17. the shielding effectiveness of practical enclosures decreases with increasing efficiency. This decrease is brought about by the fact that the enclosure is not constructed to be continuous. That is, penetrations, both deliberate and inadvertent (seams, access plates, etc), degrade the shielding effectiveness at high frequencies. It can be seen in figure 17, that, for this typical steel box, the maximum shielding effectiveness is 130 dB and occurs at 1 MHz. Within the 1-10-MHz frequency spectrum,

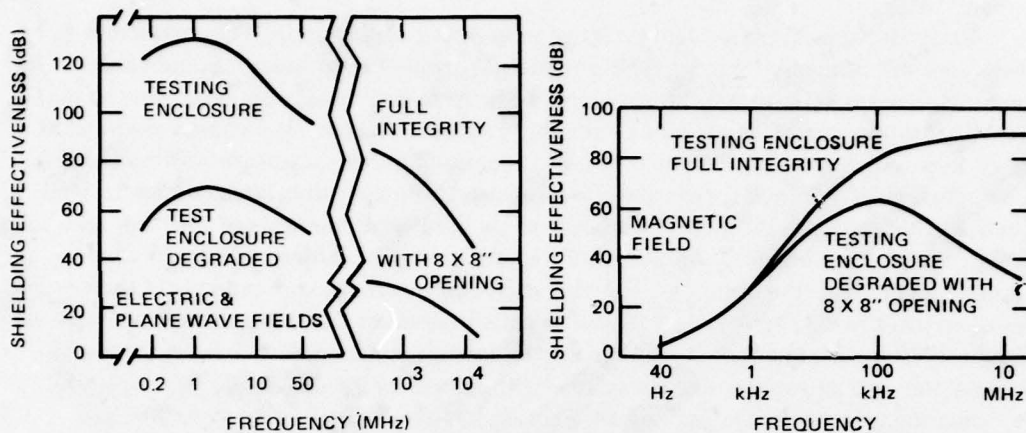


Figure 17. Shielding effectiveness of a 25.4-cm³ steel box.

where most of the EMP energy is located (fig 10), the shielding effectiveness is still high. This is not to imply, however, that the higher frequencies contained within the EMP spectrum do not present a threat. As discussed previously, the high and low portions of this spectrum, as derived from the Fourier transform of the double exponential pulse, are not representative of the real threat. These areas are highly system-dependent and are usually classified. In some cases, a significant amount of energy could be contained within them which would be attenuated less by the enclosure.

In the design or selection of the enclosure, attention should be paid to the geometric shape of the enclosure, if a choice is possible, because the enclosure represents a cavity that could have resonances at one or more of the frequencies within the coupled EMP spectrum. These resonances will be dependent not only on the geometry of the enclosure but also on its contents. Resonances at some frequencies are probably unavoidable, but the design should have them outside the data bandwidth and as small as possible; in other words, low-Q cavities.

Boxes with high-quality rf shields can be purchased from several sources. It is then important to be sure that doors or access plates are properly sealed with rf gaskets or numerous bolts or screws to ensure that the external conducting surface is continuous. If low-frequency magnetic field coupling is thought to be a problem, high-permeability shields can also be employed at the cost of added weight.

Similarly, braided wire shielded cables suffer from decreased shielding effectiveness at higher frequencies, also due to the energy leakage through the holes in the braid. Solid thin-walled tubular shielded cables do not suffer from this malady since the only means by which coupling may take place is diffusion through the walls of the tube, and this decreases with increasing frequency.

In general, cables, including FO cables, require that terminations be made at their ends. This is usually accomplished via some sort of cable connector. It is in these connections that significant leakages into enclosures may occur if the connector is not designed properly or properly installed and torqued down.

Recently, several manufacturers have introduced multibundle FO connectors to provide ease of connection for applications such as parallel data buses. Some cable connectors even provide for a solid conductor to be routed through the connectors so that power distribution may be made along with the fiber optic cables. The chassis portions of some of these connectors are designed to accept specially mounted optical sources (LEDs) and detectors (PINs). Since these connectors must provide apertures large enough to feed the entire cable through, this penetration will allow significant amounts of EMP energies to penetrate within the connector housing and the enclosure where direct electrical connections must be made to the circuitry. For this reason, it is not recommended that these types of connectors be employed in critical circuits in systems that have to survive even moderate EMP environments. If multichannel connectors are a must for a system, pig-tails from the optical sources and detectors to the enclosure walls should be employed. Also, some manufacturers are making connectors from various plastics to reduce cost. Since these connectors require relatively large apertures in the chassis which will be sources of rf penetration, they are also not recommended for use in EMP-hardened systems.

One method of reducing the EM coupling at the point at which a fiber enters an electronics box and is connected to a transmitter or receiver is to provide a conducting cylindrical sleeve for the EM energy to have to penetrate. The sleeve then becomes a waveguide with a cutoff frequency large compared to EMP frequencies of interest, and external fields are highly attenuated in traversing the waveguide (see appendix C for detailed attenuation estimates). Any electronics should be well recessed inside the enclosure, and the conducting sleeve should make good electrical connection to the conducting box wall (fiber optic connectors well torqued down).

A second probable point of entry of EM energy into a fiber optics box is through the connection to the power supply. Conducting cables will probably be used for power lines for some time, and such cables will directly penetrate the wall of a carefully shielded box. Thus, replacing signal lines by optical fibers may have little advantage for EM protection if long power lines still couple large amounts of energy into a box.

Power line coupling problems can be alleviated in several ways. The first is to minimize the EM pickup of the power line itself. As indicated in appendix A, the effective volume over which a cable collects EM energy can be reduced by minimizing the cable length and by routing the cable as near as possible to the distance from the ground plane that produces minimum coupling. We could also shield a power line and connect the shield to the ground plane at periodic intervals.

A second method of protecting against power line transients is to include some sort of interface protection at the point at which the power line enters the box. This interface protection would be designed to keep unwanted transients from coupling into system electronics. Such protection devices include various current or voltage limiters (eg, varistors, zener diodes, spark gaps, circuit breakers) and a variety of types of protective filters (band-pass filters, ferrite chokes, transformers, etc). Current and voltage limiters are essentially just fast nonlinear devices that act as switches for diverting EM signals when a certain magnitude is surpassed. Some of these limiters are difficult to use on power lines, since power line currents may keep the switch from returning to normal after a transient. Filters, on the other hand, are useful only if the EM transient has frequency content significantly different from that of the normal power line signal. This is often the case for power lines which typically are dc or very-low-frequency compared to EMP transients. Thus, in many

cases, an appropriately placed filter capacitor can simply be added to a power line circuit. The capacitor will look like a short circuit to a high-frequency transient but like an open circuit to the low-frequency power. For additional information on such protection techniques, the designer has several available sources (ref 10-12).

UPSET PROTECTION

Even though electromagnetic shielding and interface protection devices can greatly reduce the possibility of device burnout, we may still have to anticipate the functional upset of complex and sensitive circuits. The upset problem could be eliminated with additional shielding. The designer also has the option of deliberately designing his circuits to be upset-tolerant. In digital circuits, the use of higher-level logic signals and longer switching pulse lengths is one method of increasing upset tolerance. Another technique is to try to detect transients and then reset all electronics after one has been detected. (Such an automatic reset capability requires that small operational down times during transient and reset be acceptable.)

SHIELDING REQUIREMENT ESTIMATES

The systems designer will probably be presented with a particular threat and will be faced with the problem of determining how much attenuation is needed to reduce the threat to a level below the threshold with which he is concerned. To calculate the required attenuation is a simple matter; however, determining and specifying the sources of this attenuation and their magnitudes is not.

The required total shielding effectiveness (S_R) can be calculated from the basic definition as shown in eq (15) and substituting in the magnitude of the threshold level and the magnitude of the threat:

$$S_R = 20 \log [\eta] \quad (16)$$

$$\eta = \frac{|\text{threshold level}|}{|\text{threat}|}$$

where $|F(x)|$ indicates magnitude of function x . Another problem associated with using this simple expression may be expressing the magnitudes of the threat and threshold level in like terms.

The total shielding effectiveness may also be considered as the sum of two major loss mechanisms, coupling and attenuation, when they are expressed in dB. Both mechanisms may contain many individual paths, which adds to the calculational complexities. That is,

-
10. EMP Engineering and Design Principles, Bell Laboratories, Loop Transmission Division, Technical Publication Department, Whippany, NJ (1975)
 11. DNA EMP Awareness Course Notes, DNA 2772T, IIT Research Institute, October 1977
 12. Electromagnetic Pulse Handbook for Missiles and Aircraft in Flight, AFWL-TR-73-68, EMP Interaction I-1, September 1972

$$\begin{aligned}
S_R &= \sum \text{coupling loss (dB)} + \sum \text{attenuation loss (dB)} \\
&= \sum L_C + \sum S_E \quad (17)
\end{aligned}$$

The coupling losses are highly geometry-dependent, and generalities about them are usually not accurate. Therefore, they should be considered for specific system configurations when they are defined. The attenuation losses for the various constituents of the system (cables, connectors, enclosures, etc) are usually available from manufacturers. It is then only a problem of understanding their specifications and the limitations upon them.

An interesting example to work through is to determine the shielding effectiveness required for the cable of the simplistic system configuration, as presented in appendix A. Since for this case the threat was expressed in terms of energy, it is necessary to determine the amount of energy (W_C) coupled onto the cable from the incident field. In the general case, this may be found by using eq (7). For the case in which the system configuration is similar to that presented in appendix A, eq (9), which is repeated here for convenience, may be used:

$$W_C = \ell DE(t)^2 \quad (9)$$

The shielding effectiveness required by the cable may then be determined by substituting into eq (15):

$$\begin{aligned}
S_E &= 10 \log \frac{|\text{threshold level}|}{|\text{threat}|} \\
&= 10 \log \frac{|\text{threshold level}|}{DE(t)^2} - 10 \log \ell \quad * \quad (18)
\end{aligned}$$

As a specific example, consider a system in which the length of cable is 30 m and the component burnout threshold has been determined as 70 μ J. Then,

$$S_E = 10 \log \frac{7 \times 10^{-5}}{5 \times 10^{-4}} - 10 \log 30 = -23.3 \text{ dB} \quad *$$

The value for $DE(t)^2$ has been taken from figure 10 for the specific geometry of $a = 0.0253$, $h = 0.0254$. However, to keep the induced signal below that which will cause an upset (1 nJ) requires an additional 48.5-dB attenuation, or a total of -71.8-dB shielding effectiveness.

*These expressions give the energy attenuation required by the cable shielding. The manufacturers usually quote the shielding effectiveness in terms of the voltage attenuation, $20 \log n$ (dBV). For the specific example presented here, the voltage attenuation required would then be 15:1.

ELECTRO-OPTIC SYSTEM SUSCEPTIBILITY ANALYSIS

As discussed in the introduction, there are many applications for electro-optics in military aircraft systems. To limit the effort in categorizing the signal requirements for all these systems so that an analysis may be performed upon the susceptibilities of electro-optic systems to the EMP environment, the electro-optic systems have been grouped as to function and bandwidth (BW) or bit rate (BPS), as presented in table 3. This grouping has then been analyzed to determine the classes of electro-optic systems most vulnerable to EMP-induced upsets.

Table 3. Electro-optical systems data requirements and susceptibility levels.

System	Rate or Bandwidth	(SNR = 1) Power Required for Optimum Receiver (-dBm)	SNR Required (dBV)	Typical Received Optical Power (-dBm)	Design Margin (dB)	Susceptibility Level (watts)	Total Shielding Requirements ($L_C + S_E$) (-dB)
<u>Digital</u>							
Pt-Pt	1 MBPS	63	22	21	31	16×10^{-6}	116
Pt-Pt	100 MBPS	42	22	20	18	20×10^{-6}	115
Star coupler (16-port)	10 MBPS	53	22	36	6	125×10^{-9}	208
<u>Analog</u>							
Video	5-10 MHz	57	44	21	14	100×10^{-9}	167
Wideband	180 MHz	37	20	22	5	125×10^{-9}	208

The basis for the electro-optic signal requirements is derived mostly from figure 9 and typical system requirements; however, where typical systems performance specifications could be found, these were used. For the digital systems, the 22-dB SNR requirement equates to approximately a 10^{-9} bit error rate (BER). All the specifications have assumed a light-emitting diode (LED) as the optical source and a PIN diode as the photodetector, and have also assumed that <100 m of low-loss (<10 dB/km) fiber optic cable has been used. These specifications are not exact and are intended only to represent the value of typical signal levels for these classes of systems.

The susceptibility levels for the analog and digital systems have not been considered in the same manner. For the digital systems, the level was picked as that level which equaled one-half the received signal. This assumes a signal midpoint detection scheme. For the analog system, the susceptibility level was defined as that level which would increase the noise level so as to produce a 3-dB decrease in the required SNR referenced to the typical received power. Since this disturbance is a single event that recovers very quickly, this definition of susceptibility level for analog systems may be too conservative; however, this is a customary definition for analog systems.

To determine the total shielding requirements – that is, coupling losses (L_C) plus enclosure shielding effectiveness (S_E) – the threat has been taken as the peak power contained in 1 m^2 (fig 3) of the typical incident EMP pulse previously presented.

From table 3 it can be seen that the shielding requirements for analog systems are significantly greater than those for digital systems except for those multiplexed systems which incorporate star couplers with a large number of terminals (>16). This is partly due to the increased SNR requirements for analog systems over digital systems, and also partly due to the way the susceptibility level was defined, as previously pointed out. Figure 18 presents simplified block diagrams of a MIL-STD-1553 twisted shielded pair digital data transmission interface and its equivalent optical fiber interface. These are typical interfaces for an avionics data bus with a 1-MHz data requirement.

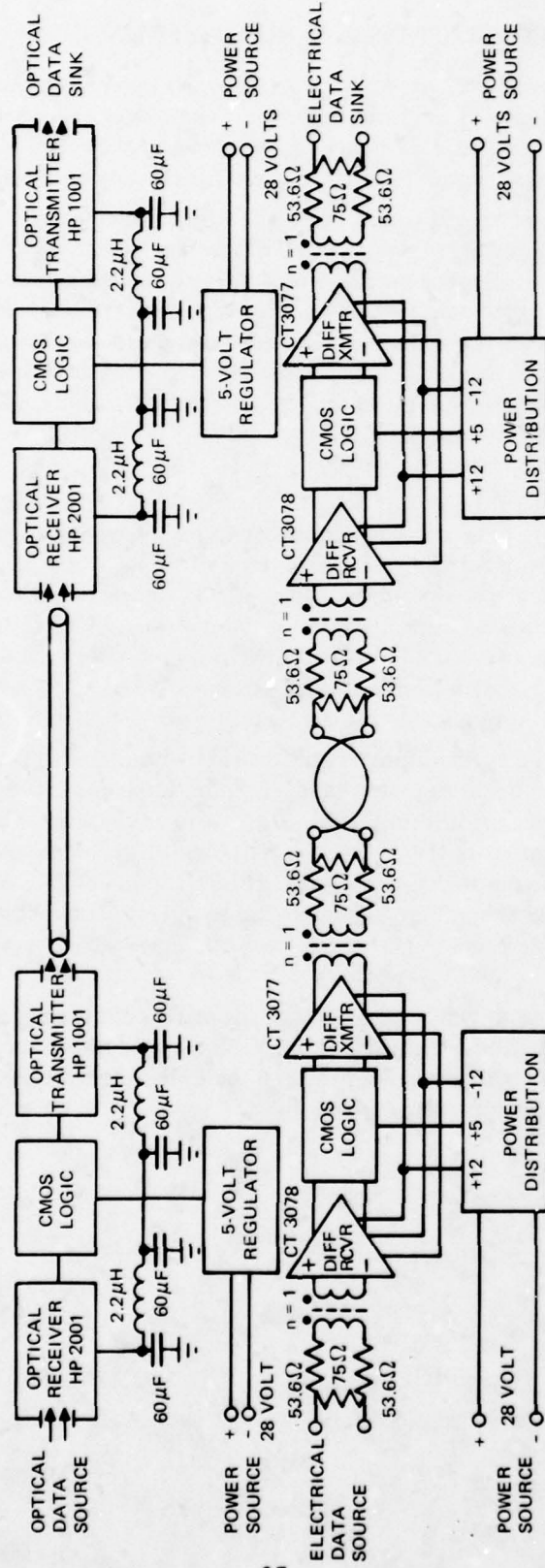


Figure 18. MIL-STD-1553 TSP and optical fiber interfaces.

CONCLUSIONS AND RECOMMENDATIONS

Methods have been presented for calculating and estimating the coupling and attenuation of various types of cables and electronic enclosures. These have been used to determine whether the incident EMP fields may be attenuated enough to reduce the energy levels coupled into the fiber optic electronics below their susceptibility levels.

It was determined that it would not be too difficult to reduce the threat levels below the component burnout thresholds ($\sim 70 \mu\text{J}$) for both electro-optic transmitter and receiver electronics — ie, following normal, good rf shielding design practices such as using shielded cabling and rf-tight boxes. However, the reduction of the threat level below the upset levels ($\sim 1 \text{ nJ}$) for the transmitter will require several orders of magnitude (50 dB) more shielding protection, and the receiver will require an additional 130 dB of shielding. The amount of protection attainable in standard military electronics, MIL-STD-461A, should protect the transmitter electronics from upsets. The receiver will require careful attention to rf integrity and circuit layout.

It can be concluded from this analysis that, even though vulnerabilities exist for unhardened electro-optic data systems operated in an EMP environment which has an incident pulse amplitude of 50 kV/m and a rise time of $\sim 5 \text{ ns}$, it is possible to provide enough protection for the system to reduce the coupled signals below the burnout and upset threshold levels for the typical integrated circuit families that are used in the implementation of electro-optic data systems. Furthermore, for those data systems that have long transmission path lengths ($>10\text{--}20 \text{ m}$), it will be easier to provide the required EMP protection for electro-optic systems than for hard-wire systems.

Analysis of a typical fiber optic connector (SMA-type) has shown that a single-fiber connector will provide more attenuation than a bundle connector (50-mil diameter). For those systems in which significant EMP fields are present at electronics box interfaces and which cannot tolerate upsets in the receiver electronics, it is recommended that the single-fiber approach be utilized in the system design. If the system design is definitely committed to the fiber optic bundle technology, pigtailling the photodetector and locating it physically away from the end of the panel mount connector will decrease the receiver upset vulnerability to EMP.

For those systems in which the power to the chassis containing electro-optic transmitters and receivers must be distributed through relatively long conductors, extra filtering on the power supply bus will be required to keep the EMP-induced transients on the power supply and ground conductors from causing upsets.

REFERENCES

1. DC Wunsch and RR Bell, Determination of Threshold Failure Levels of Semiconductor Diodes and Transistors due to Pulsed Voltages, *IEEE Trans Nucl Sci* NS-15, no 6, December 1968
2. DM Tasca, Pulsed Power Failure Modes in Semiconductors, *IEEE Trans Nucl Sci* NS-17, no 6, December 1970
3. CR Jenkins and DL Durgin, EMP Susceptibility of Integrated Circuits, *IEEE Trans Nucl Sci* NS-33, no 6, December 1975
4. C Kleiner, J Nelson, F Vassallo, and E Heaton, Integrated Circuit Model Development for EMP, *IEEE Trans Nucl Sci* NS-21, no 6, December 1974
5. Alan Allen, Noise Immunity Comparison of CMOS Versus Popular Bipolar Logic Families, Motorola Application Note AN707 (1973)
6. JA Plumer, Lighting and Electric Systems, Interface Technology Engineers Master 1978, p 188-192
7. JR Baird, Optoelectronic Aspects of Avionic Systems II, AFAL-TR-45, May 1975
8. Special Joint Issue on the Nuclear Electromagnetic Pulse, *IEEE Trans Ant Prop* AP-26, no 1, January 1978 [Also *IEEE Trans EMC*, EMC-20, no 1, February 1978]
9. CM Butler et al, Selected Topics in EMP Interaction, AFWL Interaction Notes, IN-339, August 1976
10. EMP Engineering and Design Principles, Bell Laboratories, Loop Transmission Division, Technical Publication Department, Whippany, NJ (1975)
11. DNA EMP Awareness Course Notes, DNA 2772T, IIT Research Institute, October 1977
12. Electromagnetic Pulse Handbook for Missiles and Aircraft in Flight, AFWL-TR-73-68, EMP Interaction 1-1, September 1972

APPENDIX A.
ESTIMATES OF CABLE COUPLING

Consider the configuration of two cubical electronics boxes connected by a conducting cable, as shown in figure A1. Assume the boxes are mounted on a conducting ground plane, the length of the connecting cable is ℓ , and its average height above the ground plane is h . For this simple configuration it is relatively easy to estimate the amounts of electric and magnetic field energy coupled to the box-cable system.

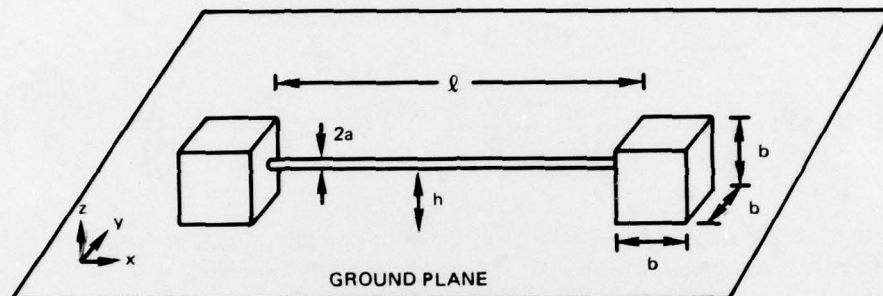


Figure A1. Model for determining effective volume.

Assume the following parameters.

E_z = average electrical field perpendicular to the ground plane

H_y = average magnetic field along the ground plane

C = capacitance per unit length of the connecting cable

L = inductance per unit length of the connecting cable

I_{sc} = circuit model short-circuit cable current

V_{oc} = circuit model open-circuit cable voltage

$P_E = I_{sc}V_{oc}$ = maximum possible power coupled to system*

h = height to the center of the cable from ground plane

a = radius of cable

$$C \approx \frac{2\pi\epsilon_0}{\cosh^{-1}\left(\frac{h}{a}\right)}$$

$$L \approx \frac{\mu_0}{2\pi} \cosh^{-1}\left(\frac{h}{a}\right)$$

*This expression gives the maximum possible power that may be attained from an electrical system. In practice, it is not possible for the short-circuit and open-circuit conditions to exist at the same time; therefore, the total power delivered by the system has to be less than this value.

E-field coupling

$$I_{sc} = C\ell Eh$$

$$V_{oc} = E_z h$$

$$P_E = Ch^2\ell EE$$

H-field coupling

$$V_{oc} = \mu_0 H_y \ell h$$

$$L\ell I_{sc} = \mu_0 H_y \ell h$$

$$\text{or } I_{sc} = \frac{\mu_0 H_y h}{L}$$

$$P_H = \frac{\mu_0^2 h^2 \ell H H}{L}$$

$$= (h^2\ell) \left(\frac{2\pi}{\cosh^{-1} \left(\frac{h}{a} \right)} \right) \frac{d}{dt} \left(\frac{\epsilon_0 E^2}{2} \right) = (h^2\ell) \left(\frac{2\pi}{\cosh^{-1} \left(\frac{h}{a} \right)} \right) \frac{d}{dt} \left(\frac{\mu_0 H^2}{2} \right)$$

Note that the final expressions for electric and magnetic power coupled to this simple box-cable system are quite similar. These expressions have been written as a volume ($h^2\ell$) times a geometric factor times the rate of change of either the electric or magnetic field energy density. We can thus think of the volume terms as being the "effective coupling volume" over which the system collects electromagnetic energy. Note that this volume is proportional to the length, ℓ , of the cable and the square of the cable height, h , above the ground plane. However, the expression does have a minimum which is a function of the ratio of h to a . We should try to route cable at this optimum distance to ground planes or make the shield an integral part of the ground plane (thus minimizing $P_{H,E}$) and also try to minimize cable lengths. Cable lengths, however, are typically comparable to overall system dimensions.

In the above estimates, the finite sizes of the electronics boxes themselves have been ignored, since such boxes are typically small and can be quite well shielded. For comparison purposes, however, we can guess that the "effective coupling volume" is of the order of the physical volume (b^3 in this case).

Consider, as an example, what typical dimensions our simple system might have if it represented the internal electronics of the aircraft. Assume $\ell \cong 20$ m, $a = b \cong 5$ cm, and $h \cong 10$ cm. The effective coupling volume due to the cable is then 1600 times that of the box. For ground systems connected by long cable lengths, this ratio would be much larger. It is thus readily apparent that replacing all conducting cables with fiber optic links has the potential of greatly reducing the effective coupling volumes.

[Note, however, that replacing only signal cables with fibers, while leaving conducting power lines, may not reduce the effective coupling volume and might even enhance power coupling.]

APPENDIX B. ELECTROMAGNETIC SHIELDING*

The most common definitions of shielding effectiveness (as used by the EMI/EMC community) are based on one region of space separated from another by a real conductor of finite thickness. The conductor is assumed to have no inadvertent or deliberate penetrations, so that any EM penetration is due to the finite skin depth to which fields will penetrate in real materials. Such idealizations are probably more appropriate to high-quality Faraday cages, such as a screen room, rather than the skin of an airplane, which will have certain penetrations.

Shielding factors are often defined in such cases as the ratio of electric or magnetic fields at a given point after and before the placement of the shield in question. Thus, the shielding factors η_E and η_M are defined by

$$\eta_E = \frac{\text{amplitude of electric field inside shielded space}}{\text{amplitude of electric field incident on shield}} \quad (\text{B1})$$

and

$$\eta_M = \frac{\text{amplitude of magnetic field inside shielded space}}{\text{amplitude of magnetic field incident on shield}} \quad (\text{B2})$$

These shielding factors are defined in terms of the incident field, which is often just assumed to be a plane wave.

The shielding effectiveness, S , is then usually defined as

$$S_E = 20 \log_{10} [1/\eta_E] \text{ dB} \quad (\text{B3})$$

and

$$S_M = 20 \log_{10} [1/\eta_M] \text{ dB} \quad (\text{B4})$$

Note that if we assume that the shield is a finite-thickness infinite plate and the incident field is a plane wave propagating perpendicularly to the surface of the plate, the shielding effectiveness, S , is just the ratio of incident energy per unit area to the energy per unit area transmitted through the sheet, all measured in dB. The factor of 20 appears because η is the ratio of fields, while power flow for a plane wave is proportional to the square of the fields.

Note also that shielding effectiveness is defined only for one particular point, although for the planar-shield geometry just mentioned it is independent of observer location. This is not the case for more complicated shielding situations. There is, thus, the question of how accurately a single parameter really is in characterizing the effectiveness of a Faraday cage.

For a semi-infinite slab of conducting material, electric fields fall off exponentially moving into the material from the surface. The exponentiation constant, δ , is known as the skin depth, where

*Much of this appendix is adapted from reference 9.

$$\delta = \frac{1}{\sqrt{\pi f \mu \sigma}} \quad (B5)$$

Here, μ and σ are permeability and conductivity, respectively, and f is the frequency of the incident wave. Penetration through a finite-thickness slab then depends upon the thickness of the slab relative to the skin depth. Slabs many skin depths thick form the best shields.

Shielding factors for a plane wave incident on a finite-thickness slab have been calculated with the result that

$$\eta_E = \eta_M = \frac{2A_0 Z_i}{2Z_0 Z_i \cosh(kd) + Z_0^2 + Z_i \sin h(kd)} \quad (B6)$$

where

$$Z_i = R_s (1 + i)$$

$$R_s = \frac{1}{\sigma \delta}$$

d = thickness of conducting slab

Z_0 = free-space impedance $\cong 377 \Omega$

The shielding effectiveness, S , calculated by using eq (B3), (B4), and (B6), is plotted in figure B1 as a function of frequency for several materials. It is clear from this figure that the shielding effectiveness of real materials decreases at low frequencies as the skin depth approaches the thickness of the slab.

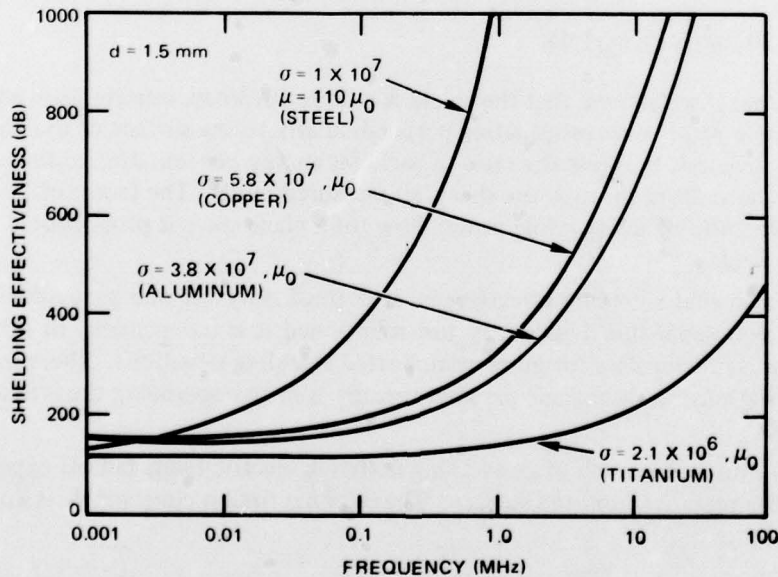


Figure B1. Shielding factor of a plane of thickness 1.5 mm of various materials (ref 9).

A convenient method of measuring shielding effectiveness, however, is to use, not plane waves, but rather two small loop antennas, as shown in figure B2. In this case, the shielding factor is defined as the ratio of voltage induced in the observer loop without the plate to that with the plate. This configuration for measuring shielding effectiveness is known as the "flat-plate magnetic shielding effectiveness" technique.

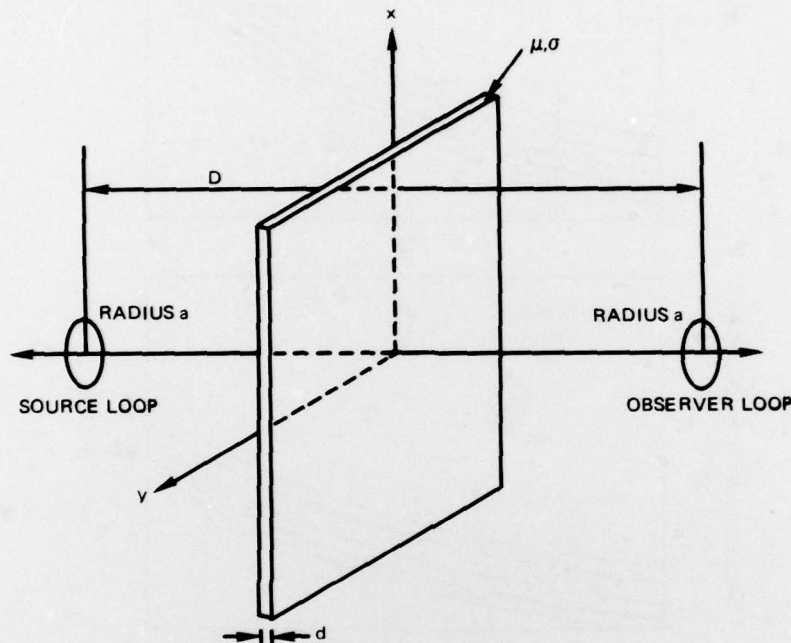


Figure B2. Shielding of a loop by a planar conductor (ref 9).

Calculated and measured shielding effectivenesses for this geometry agree well, and typical results are plotted in figure B3. Examination of these curves reveals several interesting facts. First, the shielding effectiveness, as defined for the loop geometry, is a function of loop separation in addition to the shield parameters. For example, with copper or aluminum shields, shielding effectiveness can vary by 20-30 dB, depending on whether the loops are widely separated or quite nearby.

A second important point can be noted by comparing figures B1 and B3. In all cases, the shielding effectiveness defined by the loop method is significantly smaller than that defined by plane-wave illumination. All the curves of figure B3 are below 40 dB at 10 kHz, while none of the curves in figure B1 ever fall below 100 dB.

It is clear from these examples that a single number, or even a single curve as a function of frequency, is insufficient to fully describe the shielding properties of an infinite plate of a real material of finite thickness. Results will depend upon shielding factor definitions and the method used to test shielding. The problem is obviously even more complicated when the shield is not an infinite planar conducting sheet but rather some finite-size enclosure.

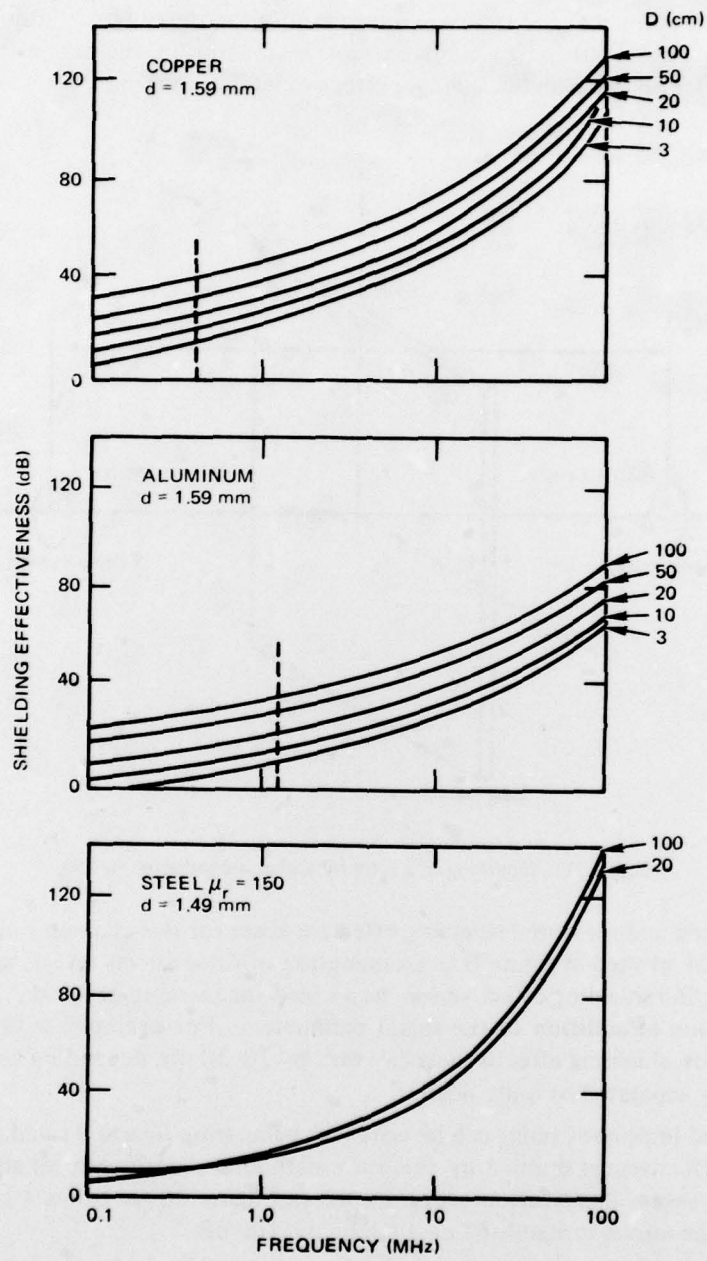


Figure B3. Shielding effectiveness of a loop by planar conductors (for configuration, see fig B2).

SHIELDING DEGRADATION DUE TO APERTURES

Electromagnetic energy can penetrate even a perfectly conducting shield through various holes or apertures. Idealized apertures might represent hatches, holes for cable bundle penetrations, access ports, or just improperly bonded metallic sections of the structure. In any case, the definitions of shielding effectiveness given above are not readily applicable to apertures, because the magnitudes of fields leaking through apertures are strongly dependent on the observer's location relative to the aperture.

An example illustrating this is shown in figure B4. This figure shows the normalized current induced on a wire inside a cylindrical cavity as a function of the distance of the wire from a small aperture. Wire current is normalized with respect to the external cylindrical skin current at the aperture if the aperture were shorted. Note that the wire current is a strong function of wire distance from the aperture. A measurement made very near the aperture would thus indicate rather poor shielding, while a measurement made some distance away would indicate very little EM penetration. How then do we define shielding effectiveness of an enclosure with apertures?

Before discussing possible methods of defining shielding effectiveness, let us first consider what is known about EM coupling through apertures. Aperture coupling has been studied for some time but is still far from being completely understood. An approximation often applicable to EMP coupling is known as Bethe's small-aperture theory. This approximation requires the aperture dimensions to be small compared to electromagnetic wavelengths of interest.

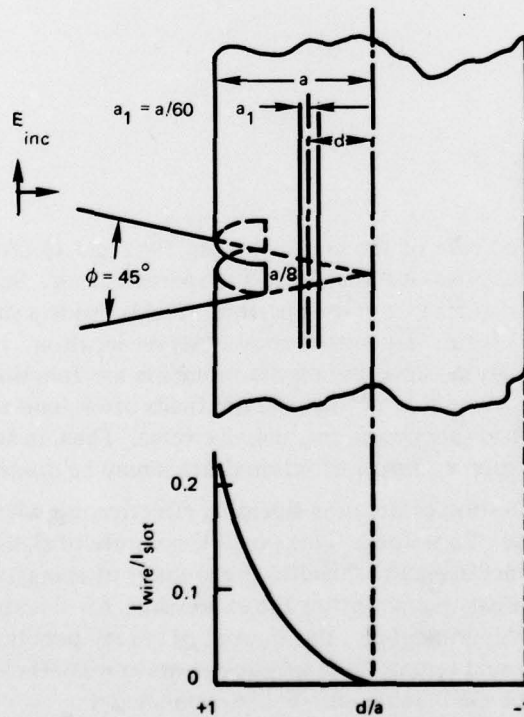


Figure. B4. Dependence of wire current on wire position within the cavity (ref 12).

To use Bethe's theory, we first calculate the skin current and charge density (ie, tangential magnetic and normal electric fields) at the location of the aperture, with the aperture shorted by a conductor. An aperture polarizability, which depends only on aperture geometry, is then calculated. The local fields at the shorted aperture are then combined with the polarizabilities to give equivalent electric and magnetic dipoles. These dipoles are the sources of the fields on the far side of the aperture (ie, the leakage fields).

As a specific example of this technique, consider a planar conductor with a circular aperture of diameter D . The short-circuit normal electric field at the aperture is assumed to be E_z , while the two components of the tangential magnetic fields are H_x and H_y . The fields on the shielded side of the planar conductor are then given in terms of an electric dipole of moment,

$$p = \epsilon \alpha_e E_z \quad , \quad (B7)$$

and two perpendicular magnetic dipoles of moments,

$$m_x = -\alpha_{m,xx} H_x \quad (B8)$$

and

$$m_y = -\alpha_{m,yy} H_y \quad (B9)$$

For a circular aperture of diameter D ,

$$\alpha_e = \frac{D^3}{12} \quad , \quad (B10)$$

while

$$\alpha_{m,xx} = \alpha_{m,yy} = \frac{D^3}{6} \quad (B11)$$

Fields on the shielded side of the conductor are thus just electric and magnetic dipole fields, at least for locations not too close to the aperture itself. Such dipole fields fall off as r^{-3} where r is the distance from the aperture. Fields inside a shielded enclosure with an aperture will thus be highly dependent upon observer location. Internal fields will also depend on aperture location, since the dipole moments are functions of external electric and magnetic fields. Note that normal electric fields often tend to be maximum where tangential magnetic fields are minimum, and vice versa. Thus, in some cases, either the electric or the magnetic dipole sources of internal fields may be dominant.

Now consider the question of defining shielding effectiveness when EM leakage is primarily due to the presence of apertures. One possible measure of shielding effectiveness is the ratio of EM energy penetrating the shield to the amount of energy incident upon it. This type of definition is roughly equivalent to the expressions for shielding effectiveness given in eq (B3) and (B4). Experimentally, the amount of energy penetrating a shield would be difficult to measure (it would require field measurements at numerous locations), but calculational estimates can be made fairly simply for certain cases.

Consider Bethe's small-aperture theory. The average power radiated by the equivalent dipoles can be written as

$$W_E = \frac{Z_0}{12\pi} c^2 k^4 p^2, \quad W_E = 10 c^2 k^4 p^2, \quad (\text{B12})$$

for an electric dipole of moment p , and

$$W_M = \frac{Z_0}{12\pi} k^4 m^2, \quad W_M = 10 k^4 m^2, \quad (\text{B13})$$

for a magnetic dipole of moment m . In these expressions, c is the speed of light, k is the wave number, and $Z_0 = 120\pi$ ohms is the impedance of free space.

These equations can then be combined with eq (B7) through (B11) to express the total EM energy that has penetrated through an aperture in terms of fields at the aperture when it is shorted. These fields can, in turn, be related to the incident fields by solving a scattering problem. As an example, consider a plane wave incident normally on an infinite planar conducting sheet with a small circular aperture of diameter D . If the aperture were shorted, the result would be a total normal electric field of zero and a total tangential magnetic field twice as large as the incident field. In this case, only the magnetic dipole term is nonzero, and the magnetic dipole moment is

$$m = \frac{D^3}{3} H_0, \quad (\text{B14})$$

where H_0 is the magnitude of the incident plane-wave magnetic field. Putting this expression into eq (B12), we can write the rate of energy flow through the aperture as

$$W = \frac{Z_0}{108\pi} k^4 D^6 H_0^2. \quad (\text{B15})$$

Now the incident power flow per unit area of the plane wave is just

$$S = 1/2 \vec{E} \times \vec{H}^* = \frac{H_0^2 Z_0}{2}. \quad (\text{B16})$$

The total power incident on the aperture is now

$$W_{in} = \frac{Z_0 H_0^2}{2} \frac{\pi D^2}{4}, \quad (\text{B17})$$

and one measure of leakage through the aperture is just the ratio of eq (B15) divided by eq (B17); ie,

$$\xi \equiv \frac{W}{W_{in}} = \frac{2(kD)^4}{27\pi^2}. \quad (\text{B18})$$

Since the aperture was assumed to be small compared to wavelengths of interest, $kD \ll 1$. The shielding factor, ξ , is thus small as long as this approximation is valid and decreases as the frequency increases. The aperture shielding effectiveness might be defined in a manner analogous to eq (B3) and (B4) so that

$$S_{AP} = -10 \log_{10}(\xi) \text{ dB} \quad (\text{B19})$$

As an example, consider a 10-MHz incident plane wave and an aperture with a diameter of 10 cm. Then $kD \approx 2 \times 10^{-2}$ and $\xi \approx 1.2 \times 10^{-9}$, giving

$$S_{AP}(F = 10 \text{ MHz}) \approx 89 \text{ dB} \quad (\text{B20})$$

A comparison of this result with figure B1 indicates that such an aperture will let much more energy penetrate the shield than the skin depth leakage due to finite conductivity.

Note that the above definition of ξ is somewhat deceiving since W_{in} was calculated only over the area of the aperture. For finite-size shields, another definition might use the entire cross-sectional area of the shield. If we assume, for example, a 1-m^2 total shield cross section with a 10-cm-diameter aperture, the ratio of aperture area to total shield cross section is about 8×10^{-3} . Using the total shield area rather than just that of the aperture would bring the shielding effectiveness given in eq (B20) up to ~ 110 dB, a result which is still far below the calculated results for solid shields.

The above discussions have not considered cavity-backed apertures or large apertures. Some studies of these issues have been carried out in the past, but we will not go into the details here. It should be noted, however, that field distributions inside a cavity driven by an aperture can be rather complex, especially at frequencies near various cavity resonances. If we happen to place a field sensor near the maximum or null of a cavity standing wave, measured results may be grossly deceptive in terms of establishing shielding effectiveness.

APPENDIX C. EM COUPLING THROUGH FIBER OPTIC CONNECTORS

The point at which a fiber enters an electronics box is a potential point of entry for EMP energy even though there is not a penetrating conductor, as in the conducting wire equivalent of a fiber optics system. The cases are different in that a conducting wire would preferentially conduct low-frequency EM energy to the inside of the box, while the penetration necessary for a fiber optics system would tend to let in primarily the high-frequency components.

The electromagnetic properties of a typical fiber optic feedthrough can probably be modeled by a hollow conducting cylinder protruding outside the electronics box wall. The fiber runs into the cylinder, where it mates to a transmitter or receiver, and the electronics leads of this equipment come out the other end of the cylinder inside the box. Such a configuration is useful for EMP protection because the small cylinder acts as a very-high-frequency waveguide. It will thus be attenuated by a factor determined by the length of the cylinder.

As a more specific example, consider the feedthrough cylinder of figure C1, which has a radius of a . Assume that the cylinder is perfectly conducting. The waveguide modes for such a cylinder are well known.* The lowest cutoff frequency occurs for the TE_{11} mode and is

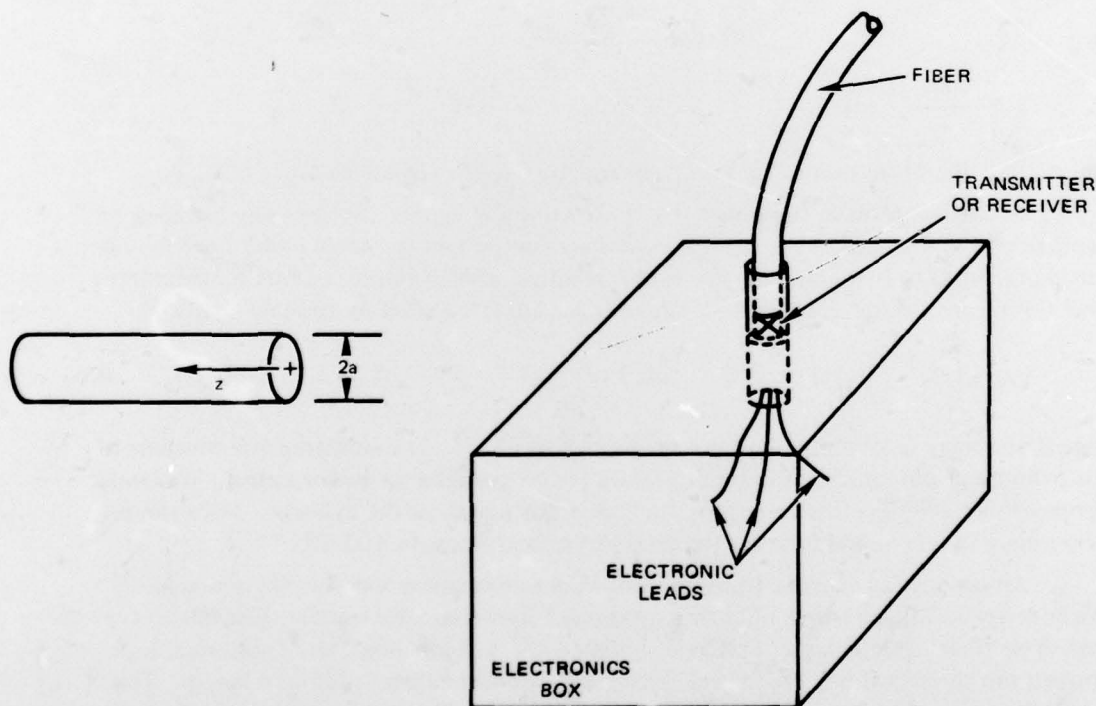


Figure C1. Schematic drawing of waveguide shield.

*See, for example, Fields and Waves in Communication Electronics, by Ramo Whinnery, and van Duzer, John Wiley & Sons (1965), section 8.04

$$f_c(\text{TE}_{11}) \cong 1.0 \times 10^{10} \text{ Hz} \quad (\text{C1})$$

The lowest cutoff frequency is thus 10 GHz for this example, and most of the EM energy from a typical EMP threat is expected to occur at frequencies far below this value.

Now, the propagation factor EM field in a waveguide is $\exp(i\omega t - \gamma z)$, where, for frequencies below cutoff,*

$$\gamma = \frac{2\pi}{\lambda_c} \sqrt{1 - (f/f_c)^2} \quad (\text{C2})$$

Waves are thus exponentially attenuated, and when frequencies of interest are far below cutoff,

$$\gamma \cong \frac{2\pi}{\lambda_c} \quad (\text{C3})$$

For this case, then, the attenuation constant, γ , is almost frequency-independent. Since, for the TE_{11} mode

$$\gamma_c = 3.41/a \quad (\text{C4})$$

then

$$\gamma \cong \frac{1.84}{a} \quad (\text{C5})$$

The result is therefore that fields are attenuated by $\exp(-1)$ in the distance of $0.54a$.

We therefore have the result that EMP coupling can be substantially reduced by lengthening the distance to the nearest electronic component (ie, the length of the cylinder outside the box) or by decreasing the cylinder radius. For example, assume that the transmitter or receiver is located at $z = 5a$. Then fields are attenuated by roughly

$$\exp - \left(\frac{1.84}{a} \right) (5a) = \exp(-9.2) \cong 1.0 \times 10^{-4} \quad (\text{C6})$$

Note that energy is attenuated by the square of this factor. The shielding effectiveness of this cylindrical waveguide is thus about 80 dB for frequencies far below cutoff. We could increase this shielding effectiveness by increasing the length of the cylinder. For example, increasing z to $10a$ would increase the shielding effectiveness to 160 dB.

An interesting exercise to work through is to determine whether there would be an advantage in using a single fiber over a typical 50-mil-diameter bundle. Consider a typical SMA-type fiber optic connector that is designed for 125- μm fiber; the cylindrical hole through the connector is 130 μm in diameter and approximately 9.8 mm in length. The cutoff frequency from eq (C1) is then 3.8×10^{11} Hz. The attenuation constant from eq (C3) is 7.96. Then the fields are attenuated by $\exp(-7.96 \times 9.8) = 1.3 \times 10^{-34}$. This is much larger than could be realized practically, since the attenuation through the enclosure walls is not this great, but it will still be small.

*Ibid, section 8.08

For the 50-mil-diameter bundle (1.27 mm) and the same length connector hole,

$$f_c = 3.9 \times 10^{10} \text{ ,}$$

$$\gamma = 0.826 \text{ ,}$$

and

$$\exp(-1.826 \times 9.8) = 3 \times 10^{-4} = 70 \text{ dB .}$$

It can be concluded that the single fiber is a better choice as far as coupling through the penetration is concerned.